Numerical solution of Maxwell's equations in axisymmetric domains with the Fourier Singular Complement Method

Patrick Ciarlet, Simon Labrunie

MATHEMATICS OF COMPUTATION
Volume 00, Number 0, Pages 000–000
S 0025-5718(XX)0000-0

NUMERICAL SOLUTION OF MAXWELL'S EQUATIONS IN AXISYMMETRIC DOMAINS WITH THE FOURIER SINGULAR COMPLEMENT METHOD

PATRICK CIARLET, JR. AND SIMON LABRUNIE

Abstract. We present an efficient method for computing numerically the solution to the time-dependent Maxwell equations in an axisymmetric domain, with arbitrary (not necessarily axisymmetric) data. The method is an extension of those introduced in [20] for Poisson's equation, and in [4] for Maxwell's equations in the fully axisymmetric setting (i.e., when the data is also axisymmetric). It is based on a Fourier expansion in the azimuthal direction, and on an improved variant of the Singular Complement Method in the meridian section. When solving Maxwell's equations, this method relies on continuous approximations of the fields, and it is both $\boldsymbol{H}(\mathbf{curl})$- and $\boldsymbol{H}(\mathrm{div})$-conforming. Also, it can take into account the lack of regularity of the solution when the domain features non-convex edges or vertices. Moreover, it can handle noisy or approximate data which fail to satisfy the continuity equation, by using either an elliptic correction method or a mixed formulation. We give complete convergence analyses for both mixed and non-mixed formulations. Neither refinements near the reentrant edges or vertices of the domain, nor cutoff functions are required to achieve the desired convergence order in terms of the mesh size, the time step and the number of Fourier modes used.

1. Introduction

There exist many methods to compute numerically the solution to Maxwell's equations. Among those methods, let us mention the edge finite element method, introduced by Nédélec [41, 42]. This method proved very efficient for the static, harmonic and eigenvalue problems related to Maxwell's equations. To improve the flexibility of the discretization, a discontinuous Galerkin method has been recently introduced [35]. On the other hand, it is interesting for some applications to have a *continuous* approximation of the electromagnetic field, aimed at capturing both the curl and the divergence of the fields. In particular, it allows to reduce the numerical noise, when the Maxwell solver is embedded in a time-dependent Vlasov–Maxwell code. This is the method earlier introduced by Heintzé *et al.* [6]. But the latter worked only in convex (curvilinear) polyhedra.

However, three-dimensional computations can be very expensive. In a number of cases, one reduces the problem to two-dimensional equations by assuming that the geometry is invariant by translation or by rotation. If in addition the data are

---

2000 *Mathematics Subject Classification.* Primary: 78M10, 65M12, 65M15; secondary: 36B65, 35L67.

Key words and phrases. Maxwell's equations, axisymmetric domains, finite element methods, mixed problems, singularities.

also invariant, then the problem can be further reduced to a single two-dimensional problem (cf. [5, 4, 24]). When this is not the case, one has to consider a series of two-dimensional problems, obtained by Fourier analysis. This approach, called the Fourier–Finite Element Method (FFEM), was initiated by Mercier–Raugel [39] for elliptic problems. More recent developments include: the works of Heinrich *et al.* [33, 34], which relied on mesh refinement techniques; and also by the authors and co-workers [19, 20], which relied on the Singular Complement Method (SCM). Both techniques allow one to improve the convergence rate of the method. Recall briefly the principle of the SCM: the space of solutions V is split *with respect to regularity* in a regular subspace V_R and a singular one V_S, namely $V = V_R \oplus V_S$. When the domain is *regular*, i.e., *convex* or with a *smooth boundary*, there is no singularity in the solutions of the Poisson or Maxwell equations, so that $V_S = \{0\}$ and $V_R = V$, and no singular complement is required. When this is not the case, one enlarges the discrete space by adding some approximation of a singular field. Combining this method with the Fourier analysis in the third dimension leads to the so-called Fourier–Singular Complement Method (FSCM).

As it is well-known, functions defined by continuous finite elements are of H^1 regularity.[1] Consequently, when solving Maxwell's equations in a non-convex and non-smooth domain, with a *continuous*, $\boldsymbol{H}(\mathbf{curl})$- *and* $\boldsymbol{H}(\mathrm{div})$-conforming discretization, the discretized spaces are always included in a closed, strict subspace V_R of V. In other words, one cannot hope to approximate the part of the field which belongs to V_S [5]. In particular, mesh refinement techniques fail. The SCM addresses this problem by explicitly adding some singular complements. An alternate choice has been devised recently by Nkemzi [43] to solve the time-harmonic Maxwell equations, which combines singular complement and mesh refinement techniques. However, the singular complement technique used in [43] requires the use of cutoff functions, which are difficult to handle numerically (due to their fast variations), as proven in [32]. Moreover, the time-dependent Maxwell equations are not easily solved when one uses mesh refinement. Finally, the generalized Maxwell equations (see [7]) which require an explicit approximation of divergence of the fields, are not covered by the theory developed in [43]. Another alternative is the Weighted Regularization Method of Costabel–Dauge [27, 28, 22], which recovers density of the discretized spaces by measuring the electromagnetic fields in appropriately weighted Sobolev spaces.

In this article, we extend the FSCM to the solution of the time-dependent Maxwell equations in an axisymmetric domain with arbitrary data. This work is a generalisation of [4], where only axisymmetric data were considered, and no convergence analysis was performed. Our analysis follows the spirit of [20], where the FSCM was applied to the solution of Poisson's equation. It also borrows the "abstract error estimate" approach from [21], where we introduced a general framework to analyse the discretisation of Maxwell's equations by nodal (continuous) finite elements, while considering several ways of taking into account the divergence condition satisfied by the fields. That is to say, the FSCM will be applied to a generalized version of Maxwell's equations, introduced in [7]. Among others, one can

[1] For any piecewise polynomial vector field $\boldsymbol{w}$ defined on $\Omega \subset \mathbb{R}^3$, the conditions $\boldsymbol{w} \in \boldsymbol{H}(\mathbf{curl};\Omega) \cap \boldsymbol{H}(\mathrm{div};\Omega)$, $\boldsymbol{w} \in H^1(\Omega)^3$, and $\boldsymbol{w} \in \mathcal{C}^0(\overline{\Omega})^3$ are equivalent.

handle data which do not satisfy the continuity equation; this is especially useful when the Maxwell solver is embedded in a Vlasov–Maxwell code.

However, this article is not a straightforward application of [21]: in the latter work, the *whole* computational domain was meshed by finite elements. Here, we use finite elements in a two-dimensional section only, and a spectral method in the third dimension. We treat the time-dependent equations, including the mixed formulations, which are used in a variety of applications in order to enforce the divergence condition. We note that one can approximate the time-harmonic equations using the approach we develop hereafter. Furthermore, we analyse the error due to the spectral analysis of the data, as in [11, 9] Finally, we propose an algorithm to implement the FSCM.

Our analysis treats the non-singular case ($V_S = \{0\}$) as a limiting case. This specific instance of the FFEM will be referred to as the Fourier–Usual Nodal Finite Element Method (FUNFEM). A Fourier–Weighted Regularisation Method could be analysed in a similar manner; this might be quite technical, as one would have to deal with *doubly* weighted Sobolev spaces. The weights inherent to the regularisation method would interact with those due to the use of cylindrical coordinates. On the other hand, edge element methods cannot be processed within the same framework. A mixed method, using edge elements conformal in a weighted $\boldsymbol{H}(\mathbf{curl})$-type space to solve the static Maxwell equations with axisymmetric data, was described and analysed in [24]. In order to analyse a Fourier–Edge Element Method for time-dependent Maxwell equations, one would have to combine this approach with that of [23], as well as Fourier analysis.

The outline of the article is as follows. In section 2, we present the geometrical setting, the various versions of the Maxwell equations which we study, as well as the variational formulations in three dimensions and two dimensions. Then, in section 3, we analyse the impact of the numerical Fourier analysis and truncation. Next, in section 4, we provide mode-wise, abstract (method-independent) error estimates. Section 5 describes the singularities of electromagnetic fields, and the theoretical foundations of the (F)SCM. Practical approximation results are then obtained in section 6. Section 7 discusses a possible implementation of the FSCM.

2. Equations and dimension reduction

2.1. **Geometric setting and notations.** In this article, we consider an *axisymmetric domain* Ω, generated by the rotation of a polygon ω around one of its sides, denoted γ_a. The boundary of ω is thus $\partial\omega = \gamma_a \cup \gamma_b$, where γ_b generates the boundary Γ of Ω. We assume for simplicity that the domain Ω is simply connected, with a connected boundary. The natural cylindrical coordinates will be denoted by (r, θ, z). The geometrical singularities that may occur on Γ are circular edges and conical vertices, which correspond respectively to off-axis corners of γ_b and to its extremities. Figure 1 shows the various notations associated to these singularities; a more complete description of the geometry of ω can be found in [2, 3].

As we know from these references, the initial- and boundary-value problems associated with the (static or time-dependent) Maxwell equations will be singular, i.e. their solution will generically not be in $\boldsymbol{H}^1(\Omega)$ — as it would be the case in

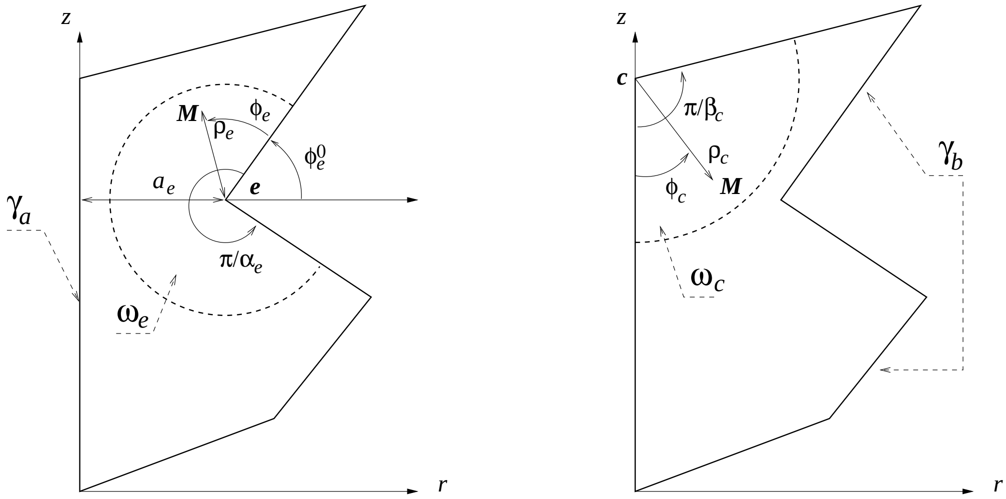

FIGURE 1. Notations for the geometrical singularities; $\boldsymbol{e}$: reentrant edge; $\boldsymbol{c}$: conical vertex.

a regular[2] domain — iff there are reentrant edges or *sharp* vertices in Γ. Sharp vertices are defined by the condition (see Figure 1):

$$\nu_c < \frac{1}{2}, \quad \text{where: } \nu_c := \min\left\{\nu > 0 : P_\nu\left(\cos\frac{\pi}{\beta_c}\right) = 0\right\}, \tag{2.1}$$

and P_ν denotes the Legendre function. This is satisfied iff $\pi/\beta_c > \pi/\beta_\star \simeq 130°48'$.

We define the comparison operators $\lesssim$ and $\approx$ as follows. $a \lesssim b$ means $a \le C\, b$, where C is a constant which depends *only* on the geometry, and *not* on the mesh size h, the Fourier order k, or the data of the Maxwell problem. $a \approx b$ denotes the conjunction of $a \lesssim b$ and $b \lesssim a$.

2.2. **Three-dimensional equations.** We start from the classical Maxwell equations in vacuum:

$$\begin{aligned}
\frac{\partial \boldsymbol{E}}{\partial t} - c^2\, \mathbf{curl}\, \boldsymbol{B} &= -\frac{\boldsymbol{J}}{\varepsilon_0},\\
\frac{\partial \boldsymbol{B}}{\partial t} + \mathbf{curl}\, \boldsymbol{E} &= 0,\\
\operatorname{div} \boldsymbol{E} &= \frac{\varrho}{\varepsilon_0},\\
\operatorname{div} \boldsymbol{B} &= 0.
\end{aligned}$$

Let $\boldsymbol{n}$ denote the unit outward normal vector to the boundary, and assume that the domain in which we solve Maxwell's equations is surrounded by a perfect conductor, which imposes,

$$\boldsymbol{E} \times \boldsymbol{n} = 0 \text{ and } \boldsymbol{B} \cdot \boldsymbol{n} = 0 \text{ on } \Gamma. \tag{2.2}$$

The initial condition is simply

$$(\boldsymbol{E}, \boldsymbol{B})_{|t=0} = (\boldsymbol{E}_0, \boldsymbol{B}_0), \tag{2.3}$$

[2]Recall that a domain is regular if it is convex or if its boundary belongs to $\mathcal{C}^{1,1}$.

for some given data $(\boldsymbol{E}_0, \boldsymbol{B}_0)$. A necessary condition for these equations to be well-posed is the continuity equation

$$\operatorname{div} \boldsymbol{J} + \frac{\partial \varrho}{\partial t} = 0. \tag{2.4}$$

Remark 2.1. One can extend our results to the case of composite materials (see [29, 37, 38, 22] for the treatment of singularities at the interfaces), or impose a Silver-Müller absorbing boundary condition on a part of the boundary. For the latter, see for instance [5, 4, 11].

In order to develop efficient finite element methods in our setting, it is preferable to use equivalent second order formulations. Eliminating $\boldsymbol{E}$ and $\boldsymbol{B}$ between the evolution equations, one finds that the electric and magnetic fields satisfy the following vector wave equations

$$\frac{\partial^2 \boldsymbol{E}}{\partial t^2} + c^2 \,\mathbf{curl}\,\mathbf{curl}\,\boldsymbol{E} = -\frac{1}{\varepsilon_0}\frac{\partial \boldsymbol{J}}{\partial t}, \tag{2.5}$$

$$\frac{\partial^2 \boldsymbol{B}}{\partial t^2} + c^2 \,\mathbf{curl}\,\mathbf{curl}\,\boldsymbol{B} = \frac{1}{\varepsilon_0}\,\mathbf{curl}\,\boldsymbol{J}. \tag{2.6}$$

The constraint equations (divergence and boundary conditions) still hold; moreover, one has to supply the second-order problem with initial conditions for the time derivatives:

$$\frac{\partial \boldsymbol{E}}{\partial t}_{|t=0} = \boldsymbol{E}_1, \text{ where } \boldsymbol{E}_1 = c^2\,\mathbf{curl}\,\boldsymbol{B}_0 - \frac{1}{\varepsilon_0}\boldsymbol{J}_{|t=0}, \tag{2.7}$$

$$\frac{\partial \boldsymbol{B}}{\partial t}_{|t=0} = \boldsymbol{B}_1, \text{ where } \boldsymbol{B}_1 = -\,\mathbf{curl}\,\boldsymbol{E}_0, \tag{2.8}$$

and the extra boundary condition for the magnetic field:

$$\left(c^2\,\mathbf{curl}\,\boldsymbol{B} - \frac{1}{\varepsilon_0}\boldsymbol{J}\right) \times \boldsymbol{n} = 0.$$

As they only involve the curl operator, the equations (2.5) and (2.6) are adapted to discretisations by edge elements [23, 40]. If one wishes to use nodal finite elements — which are generally more efficient for charged particle simulations, especially Vlasov–Maxwell computations — one has to add terms related to the divergence of the fields [6, 5, 4], yielding the "augmented" formulations:

$$\frac{\partial^2 \boldsymbol{E}}{\partial t^2} + c^2 \left(\mathbf{curl}\,\mathbf{curl}\,\boldsymbol{E} - \mathbf{grad}\operatorname{div}\boldsymbol{E}\right) = -\frac{1}{\varepsilon_0}\frac{\partial \boldsymbol{J}}{\partial t} - \frac{c^2}{\varepsilon_0}\,\mathbf{grad}\,\varrho, \tag{2.9}$$

$$\frac{\partial^2 \boldsymbol{B}}{\partial t^2} + c^2 \left(\mathbf{curl}\,\mathbf{curl}\,\boldsymbol{B} - \mathbf{grad}\operatorname{div}\boldsymbol{B}\right) = \frac{1}{\varepsilon_0}\,\mathbf{curl}\,\boldsymbol{J}. \tag{2.10}$$

Remark 2.2. In the time-harmonic regime, the addition of **grad** div terms is usually called "regularization", see among others [14, 26, 27, 15].

If one wants the divergence constraints to be explicitly preserved in time, even though the data may not satisfy exactly (a discrete version of) the continuity equation (2.4), one can use "mixed" or saddle-point formulations. Here are the mixed augmented versions:

$$\frac{\partial^2 \boldsymbol{E}}{\partial t^2} + c^2 \left(\mathbf{curl}\,\mathbf{curl}\,\boldsymbol{E} - \mathbf{grad}\,\mathrm{div}\,\boldsymbol{E}\right) + \mathbf{grad}\,P_E = -\frac{1}{\varepsilon_0}\frac{\partial \boldsymbol{J}}{\partial t} - \frac{c^2}{\varepsilon_0}\,\mathbf{grad}\,\varrho, \tag{2.11}$$

$$\mathrm{div}\,\boldsymbol{E} = \frac{\varrho}{\varepsilon_0}\,; \tag{2.12}$$

$$\frac{\partial^2 \boldsymbol{B}}{\partial t^2} + c^2 \left(\mathbf{curl}\,\mathbf{curl}\,\boldsymbol{B} - \mathbf{grad}\,\mathrm{div}\,\boldsymbol{B}\right) + \mathbf{grad}\,P_B = \frac{1}{\varepsilon_0}\,\mathbf{curl}\,\boldsymbol{J}, \tag{2.13}$$

$$\mathrm{div}\,\boldsymbol{B} = 0. \tag{2.14}$$

The mixed unaugmented versions simply lack the **grad** div terms. Setting $P = -c^2\,\partial_t p$, one obtains a *formulation with elliptic correction* [7] which does not have a saddle-point structure, but actually is a non-mixed formulation with a modified right-hand side devised to take into account the lack of charge conservation. It can be studied much like the formulations (2.5)–(2.6) or (2.9)–(2.10), with *ad hoc* hypotheses [21].

In the sequel, we shall concentrate on the various augmented formulations for the electric field, and mention along the way the adaptations for the magnetic field. For the sake of simplicity, we also set $c = \varepsilon_0 = 1$.

2.3. **Variational formulations in 3D.** Consider $L^2(\Omega)$ the Lebesgue space of measurable and square integrable functions over Ω, with $(\cdot \mid \cdot)$ and $\|\cdot\|_0$ its associated scalar product and norm, $H^s(\Omega)$ the scale of Sobolev spaces, for $s \in \mathbb{R}$, and $\overset{\circ}{H}{}^1(\Omega)$ the subspace of $H^1(\Omega)$ made of elements with a vanishing trace on $\Gamma = \partial\Omega$. From now on, we adopt the notations $\boldsymbol{L}^2(\Omega) = L^2(\Omega)^3$, $\boldsymbol{H}^s(\Omega) = H^s(\Omega)^3$ and $\underline{H}^s(\Omega) := \bigcap_{\sigma<s} H^\sigma(\Omega)$, $\underline{\boldsymbol{H}}^s(\Omega) := \bigcap_{\sigma<s} \boldsymbol{H}^\sigma(\Omega)$.

The electric field naturally belongs to the Sobolev space $\boldsymbol{H}_0(\mathbf{curl};\Omega)$, where

$$\boldsymbol{H}(\mathbf{curl};\Omega) := \{\boldsymbol{v} \in \boldsymbol{L}^2(\Omega)\ :\ \mathbf{curl}\,\boldsymbol{v} \in \boldsymbol{L}^2(\Omega)\}\ ,$$
$$\boldsymbol{H}_0(\mathbf{curl};\Omega) := \{\boldsymbol{v} \in \boldsymbol{H}(\mathbf{curl};\Omega)\ :\ \boldsymbol{v} \times \boldsymbol{n}_{|\Gamma} = 0\}.$$

At the same time, the augmented formulation, as described in Assous *et al.* [6], is set in the functional space

$$\boldsymbol{X}(\Omega) := \boldsymbol{H}_0(\mathbf{curl};\Omega) \cap \boldsymbol{H}(\mathrm{div};\Omega),$$
$$\text{where:}\quad \boldsymbol{H}(\mathrm{div};\Omega) := \{\boldsymbol{v} \in \boldsymbol{L}^2(\Omega)\ :\ \mathrm{div}\,\boldsymbol{v} \in L^2(\Omega)\}.$$

The space $\boldsymbol{X}(\Omega)$ is compactly embedded in $\boldsymbol{L}^2(\Omega)$ [44]. As a consequence, when Γ is connected, one can define an equivalent scalar product and norm on $\boldsymbol{X}(\Omega)$, as

$$a(\boldsymbol{u},\boldsymbol{v}) := (\mathbf{curl}\,\boldsymbol{u} \mid \mathbf{curl}\,\boldsymbol{v}) + (\mathrm{div}\,\boldsymbol{u} \mid \mathrm{div}\,\boldsymbol{v}), \quad \|\boldsymbol{u}\|_{\boldsymbol{X}} := a(\boldsymbol{u},\boldsymbol{u})^{1/2}.$$

In other words, the L^2-norm is uniformly bounded by the $\boldsymbol{X}$-norm for elements of $\boldsymbol{X}(\Omega)$: this is the so-called Weber inequality.

In [21] we noticed that the vector wave equation (2.9) satisfied by the electric field can be recast in the form:
Find $\boldsymbol{E} \in H^1(0,T;\boldsymbol{L}^2(\Omega)) \cap L^2(0,T;\boldsymbol{X}(\Omega))$ *such that*

$$\frac{d^2}{dt^2}(\boldsymbol{E}(t) \mid \boldsymbol{F}) + a(\boldsymbol{E}(t),\boldsymbol{F}) = (\boldsymbol{\psi}(t) \mid \boldsymbol{F}), \quad \forall \boldsymbol{F} \in \boldsymbol{X}(\Omega). \tag{2.15}$$

Above, we have set: $(\boldsymbol{\psi} \mid \boldsymbol{F}) = -(\partial_t \boldsymbol{J} \mid \boldsymbol{F}) + (\varrho \mid \operatorname{div} \boldsymbol{F})$, i.e., $\boldsymbol{\psi} := -\partial_t \boldsymbol{J} - \mathbf{grad}\, \varrho$. In this article, we shall always assume that $\boldsymbol{\psi}$ belongs to $L^2(0,T;\boldsymbol{L}^2(\Omega))$; so the equation (2.15) admits a unique solution $\boldsymbol{E} \in \mathcal{C}^0(0,T;\boldsymbol{X}(\Omega)) \cap \mathcal{C}^1(0,T;\boldsymbol{L}^2(\Omega)) \cap H^2(0,T;\boldsymbol{X}(\Omega)')$ by the Lions variational theory [36]. This is the case if, e.g., $\boldsymbol{J} \in H^1(0,T;\boldsymbol{L}^2(\Omega))$ and $\varrho \in L^2(0,T;\overset{\circ}{H}{}^1(\Omega))$.

As far as the magnetic field is concerned, it is worth noting that the formulation (2.10) does not belong in the framework of the Lions theory. Moreover, some underlying integrations by parts and certain traces considered are not justified *a priori*. The well-posedness can be proved by following [10].

The mixed augmented formulation is given as:
Find $\boldsymbol{E} \in H^1(0,T;\boldsymbol{L}^2(\Omega)) \cap L^2(0,T;\boldsymbol{X}(\Omega))$ *and* $P \in L^2(0,T;L^2(\Omega))$ *such that*

$$\frac{d^2}{dt^2}(\boldsymbol{E}(t) \mid \boldsymbol{F}) + a(\boldsymbol{E}(t),\boldsymbol{F}) + b(\boldsymbol{F},P(t)) = (\boldsymbol{\psi}(t) \mid \boldsymbol{F}), \quad \forall \boldsymbol{F} \in \boldsymbol{X}(\Omega), \tag{2.16}$$

$$b(\boldsymbol{E}(t),q) = (\varrho(t) \mid q), \quad \forall q \in L^2(\Omega). \tag{2.17}$$

where we have set: $b(\boldsymbol{v},q) := (q \mid \operatorname{div} \boldsymbol{v})$. As remarked in [21], the well-posedness result proved in [17, 7] for the mixed unaugmented formulation can be easily generalised to the mixed augmented one.

We complete this paragraph with a simple, but useful continuity result.

Proposition 2.3. *Assume that* $\boldsymbol{J} \in H^{m+1}(0,T;\boldsymbol{L}^2(\Omega))$ *and* $\varrho \in H^m(0,T;\overset{\circ}{H}{}^1(\Omega))$, *for some* $m \in \mathbb{N}$. *Then the solution to the augmented formulation has the regularity* $\boldsymbol{E} \in \mathcal{C}^m(0,T;\boldsymbol{X}(\Omega)) \cap \mathcal{C}^{m+1}(0,T;\boldsymbol{L}^2(\Omega))$, *and satisfies the continuity estimate:*

$$\|\partial_t^{m+1}\boldsymbol{E}(t)\|_0 + \|\partial_t^m \boldsymbol{E}(t)\|_{\boldsymbol{X}} \lesssim \|\boldsymbol{J}\|_{H^{m+1}(0,t;\boldsymbol{L}^2(\Omega))} + \|\varrho\|_{H^m(0,t;\overset{\circ}{H}{}^1(\Omega))}. \tag{2.18}$$

Similarly, if $\boldsymbol{J} \in H^{m+1}(0,T;\boldsymbol{L}^2(\Omega))$ *and* $\varrho \in \mathcal{C}^m(0,T;L^2(\Omega)) \cap H^{m+2}(0,T;H^{-1}(\Omega))$, *then the solution to the mixed augmented formulation has the regularity* $\boldsymbol{E} \in \mathcal{C}^m(0,T;\boldsymbol{X}(\Omega)) \cap \mathcal{C}^{m+1}(0,T;\boldsymbol{L}^2(\Omega))$, $P \in \mathcal{C}^m(0,T;L^2(\Omega))$, *with the continuity estimate:*

$$\begin{aligned} &\|\partial_t^{m+1}\boldsymbol{E}(t)\|_0 + \|\partial_t^m \boldsymbol{E}(t)\|_{\boldsymbol{X}} + \|\partial_t^m P(t)\|_0 \\ &\quad \lesssim \quad \|\boldsymbol{J}\|_{H^{m+1}(0,t;\boldsymbol{L}^2(\Omega))} + \|\varrho\|_{\mathcal{C}^m(0,t;L^2(\Omega)) \cap H^{m+2}(0,t;H^{-1}(\Omega))}. \end{aligned} \tag{2.19}$$

Proof. If $m = 0$, these are the classical well-posedness results, see [36, 17, 7]. In the general case, the above assumptions ensure that the variational formulations are well-posed with $\boldsymbol{J}$ and ϱ replaced with $\partial_t^m \boldsymbol{J}$ and $\partial_t^m \varrho$; therefore, they have a unique solution satisfying the classical continuity estimate. Yet, this solution satisfies the same equations (in the sense of distributions) as $\partial_t^m \boldsymbol{E}$ or $(\partial_t^m \boldsymbol{E}, \partial_t^m P)$; we conclude by the uniqueness of the temperate solution to a linear equation. □

2.4. **Functional spaces in 2D.** The scalar and vector fields defined on Ω will be characterised through their Fourier series in θ, the coefficients of which are functions defined on ω, viz.

$$w(r,\theta,z) = \frac{1}{\sqrt{2\pi}} \sum_{k\in\mathbb{Z}} w^k(r,z)\, \mathrm{e}^{\mathrm{i}k\theta}, \text{ resp. } \boldsymbol{w}(r,\theta,z) = \frac{1}{\sqrt{2\pi}} \sum_{k\in\mathbb{Z}} \boldsymbol{w}^k(r,z)\, \mathrm{e}^{\mathrm{i}k\theta},$$

and the truncated Fourier expansion of $\boldsymbol{w}$ at order N is:

$$\boldsymbol{w}^{[N]}(r,\theta,z) = \frac{1}{\sqrt{2\pi}} \sum_{k=-N}^{N} \boldsymbol{w}^k(r,z)\, \mathrm{e}^{\mathrm{i}k\theta}. \tag{2.20}$$

The regularity of the function w (resp. $\boldsymbol{w}$) in the scale $H^s(\Omega)$ (resp. $\boldsymbol{H}^s(\Omega)$), for $s \geq 0$, can be characterised by that of the $(w^k)_{k\in\mathbb{Z}}$ (resp. the cylindrical components of the $(\boldsymbol{w}^k)_{k\in\mathbb{Z}}$: $\boldsymbol{w}^k = w_r^k \mathbf{e}_r + w_\theta^k \mathbf{e}_\theta + w_z^k \mathbf{e}_z$) in certain spaces of functions defined over ω [12, §§II.1 to II.3], namely:

$$w \in H^s(\Omega) \iff \forall k \in \mathbb{Z},\ w^k \in H^s_{(k)}(\omega) \quad \text{and} \quad \sum_{k\in\mathbb{Z}} \|w^k\|^2_{H^s_{(k)}(\omega)} < \infty,$$

$$\boldsymbol{w} \in \boldsymbol{H}^s(\Omega) \iff \forall k \in \mathbb{Z},\ \boldsymbol{w}^k \in \boldsymbol{H}^s_{(k)}(\omega) \quad \text{and} \quad \sum_{k\in\mathbb{Z}} \|\boldsymbol{w}^k\|^2_{\boldsymbol{H}^s_{(k)}(\omega)} < \infty,$$

where the $H^s_{(k)}(\omega)$ and $\boldsymbol{H}^s_{(k)}(\omega)$ are defined in turn with the help of two different types of weighted Sobolev spaces. We shall now give these definitions for the values of s and k chiefly needed in this article. The notations for the various spaces are the same as in [12], where the interested reader can find the proofs and the most general versions of the subsequent statements.[3]

First, for any $\tau \in \mathbb{R}$ we consider the weighted Lebesgue space

$$L^2_\tau(\omega) := \left\{ w \text{ measurable on } \omega : \iint_\omega |w(r,z)|^2\ r^\tau\, \mathrm{d}r\, \mathrm{d}z < \infty \right\}.$$

This space, as well as all the spaces introduced in this article, is a Hermitian space of functions with *complex* values. The scale $\left(H^s_\tau(\omega)\right)_{s\geq 0}$ is the canonical Sobolev scale built upon $L^2_\tau(\omega)$, defined for $s \in \mathbb{N}$ as:

$$H^s_\tau(\omega) := \left\{ w \in L^2_\tau(\omega) : \partial_r^\ell \partial_z^m w \in L^2_\tau(\omega),\ \forall \ell, m \text{ s.t. } 0 \leq \ell + m \leq s \right\},$$

and by interpolation for $s \notin \mathbb{N}$. We denote by $\|\cdot\|_{s,\tau}$ and $|\cdot|_{s,\tau}$ the canonical norm and semi-norm of $H^s_\tau(\omega)$. We also define the subspace $\overset{\diamond}{H}{}^1_1(\omega)$ (of $H^1_1(\omega)$) of functions which vanish on γ_b: it is involved in the definition of the Fourier coefficients of functions in $\overset{\circ}{H}{}^1(\Omega)$.

A prominent role will be played by $L^2_1(\omega)$, which appears to be the space of Fourier coefficients (at all modes) of functions in $L^2(\Omega)$; thus its scalar product is also denoted $(\cdot \mid \cdot)$. Upon this space, we build another, dimensionally homogeneous Sobolev scale $\left(V^s_1(\omega)\right)_{s\geq 0}$, defined as:

$$V^s_1(\omega) := \left\{ w \in H^s_1(\omega) : r^{\ell+m-s}\, \partial_r^\ell \partial_z^m w \in L^2_1(\omega),\ \forall \ell, m \text{ s.t. } 0 \leq \ell + m \leq \lfloor s \rfloor \right\},$$

where $\lfloor s \rfloor$ denotes the integral part of s. One can check that the general definition reduces to

$$V^s_1(\omega) = \left\{ w \in H^s_1(\omega) : \partial_r^j w\big|_{\gamma_a} = 0, \text{ for all } j \in \mathbb{N} \text{ s.t. } j < s - 1 \right\},$$

when s is not an integer; while for the first values of $s \in \mathbb{N}$, we have:

$$V^0_1(\omega) = L^2_1(\omega), \qquad V^1_1(\omega) = H^1_1(\omega) \cap L^2_{-1}(\omega), \qquad V^2_1(\omega) = H^2_1(\omega) \cap H^1_{-1}(\omega).$$

The canonical norm of $V^s_1(\omega)$ is denoted by $|||\cdot|||_{s,1}$; it is equivalent to $|\cdot|_{s,1}$ except for $s \in \mathbb{N} \setminus \{0\}$.

---

[3]Much of this subsection parallels [43, §§2.2 to 2.4]. However, our statements are more general than those of the latter work, which uses different notations for the weighted spaces, as in [39, 33].

We are now ready to define the most useful spaces of Fourier coefficients.

Proposition 2.4. *The spaces $H^s_{(k)}(\omega)$, for $s \in [0,2]$, are characterised as follows.*

$$\begin{aligned}
\forall s \in [0,1) :\ & H^s_{(k)}(\omega) = H^s_1(\omega),\ \forall k\,;\\
\forall s \in [1,2) :\ & H^s_{(0)}(\omega) = H^s_1(\omega),\\
& H^s_{(k)}(\omega) = V^s_1(\omega),\ \forall |k| \ge 1\,;\\
s = 2 :\quad & H^2_{(0)}(\omega) = \left\{ w \in H^2_1(\omega) : \partial_r w \in L^2_{-1}(\omega) \right\},\\
& H^2_{(\pm 1)}(\omega) = \left\{ w \in H^2_1(\omega) : w|_{\gamma_a} = 0 \right\},\\
& H^2_{(k)}(\omega) = V^2_1(\omega),\ \forall |k| \ge 2.
\end{aligned}$$

Remark 2.5. The scales $H^s_1(\omega)$, $V^s_1(\omega)$, and $H^s_{(k)}(\omega)$ (for all k) can be extended to negative values of the exponent s, by the usual duality procedure with respect to the pivot space, which is $L^2_1(\omega)$ in all cases. Thus the $H^s_{(k)}(\omega)$, for $s < 0$, appear as the spaces of Fourier coefficients of functions in $H^s(\Omega)$, see §3 below.

Proposition 2.6. *The spaces $\boldsymbol{H}^s_{(k)}(\omega)$, for $0 \le s < 2$, are characterised as follows.*

$$\begin{aligned}
s = 0 :\quad & \boldsymbol{H}^0_{(k)}(\omega) = \boldsymbol{L}^2_1(\omega) := L^2_1(\omega)^3,\ \forall k\,;\\
\forall s \in (0,1) :\ & \boldsymbol{H}^s_{(k)}(\omega) = H^s_1(\omega)^3,\ \forall k\,;\\
s = 1 :\quad & \boldsymbol{H}^1_{(0)}(\omega) = V^1_1(\omega) \times V^1_1(\omega) \times H^1_1(\omega),\\
& \boldsymbol{H}^1_{(\pm 1)}(\omega) = \left\{ (w_r, w_\theta, w_z) \in H^1_1(\omega) \times H^1_1(\omega) \times V^1_1(\omega) : w_r \pm \mathrm{i}\, w_\theta \in L^2_{-1}(\omega) \right\},\\
& \boldsymbol{H}^1_{(k)}(\omega) = V^1_1(\omega)^3,\ \forall |k| \ge 2\,;\\
\forall s \in (1,2) :\ & \boldsymbol{H}^s_{(0)}(\omega) = V^s_1(\omega) \times V^s_1(\omega) \times H^s_1(\omega),\\
& \boldsymbol{H}^s_{(\pm 1)}(\omega) = \left\{ (w_r, w_\theta, w_z) \in H^s_1(\omega) \times H^s_1(\omega) \times V^s_1(\omega) :\ w_r \pm \mathrm{i}\, w_\theta \big|_{\gamma_a} = 0 \right\},\\
& \boldsymbol{H}^s_{(k)}(\omega) = V^s_1(\omega)^3,\ \forall |k| \ge 2.
\end{aligned}$$

For $|k| < s$, the space $\boldsymbol{H}^s_{(k)}(\omega)$ is endowed with the natural norm $\|\cdot\|_{s,(k)}$ given by the above definition, while for $|k| \ge s$ the canonical norm is:

$$\|\boldsymbol{w}\|^2_{s,(k)} = \|\boldsymbol{w}\|^2_{s,1} + |k|^{2s}\, \|r^{-s}\, \boldsymbol{w}\|^2_{0,1}. \tag{2.21}$$

With this definition, there holds the equivalence of norms:

$$\|\boldsymbol{w}\|^2_{\boldsymbol{H}^s(\Omega)} \approx \sum_{k \in \mathbb{Z}} \|\boldsymbol{w}^k\|^2_{s,(k)}\,.$$

Remark 2.7. In order to take into account the conditions on γ_a for the modes $k = \pm 1$, we shall sometimes use the following representation for the vector fields in $\boldsymbol{H}^s_{(\pm 1)}(\omega)$: $\boldsymbol{w} = w_+\, \mathbf{e}_+ + w_-\, \mathbf{e}_- + w_z\, \mathbf{e}_z$, with $w_\pm = \frac{1}{\sqrt{2}}\,(w_r \mp \mathrm{i}\, w_\theta)$ and $\mathbf{e}_\pm = \frac{1}{\sqrt{2}}\,(\mathbf{e}_r \pm \mathrm{i}\, \mathbf{e}_\theta)$. Thus, $\boldsymbol{w} \in \boldsymbol{H}^1_{(1)}(\omega)$ has a component w_+ on γ_a, while w_- vanishes in a weak sense [2, Proposition 3.18]; and conversely for $\boldsymbol{w} \in \boldsymbol{H}^1_{(-1)}(\omega)$.

Let us now examine the space of relevant Fourier coefficients for the electromagnetic fields. One easily checks that for $w \in H^1(\Omega)$, resp. $w \in L^2(\Omega)$ such that $\Delta w \in L^2(\Omega)$, there holds:

$$\mathbf{grad}\, w = \frac{1}{\sqrt{2\pi}} \sum_{k \in \mathbb{Z}} \mathbf{grad}_k\, w^k\, \mathrm{e}^{\mathrm{i}k\theta}, \quad \text{resp.} \quad \Delta w = \frac{1}{\sqrt{2\pi}} \sum_{k \in \mathbb{Z}} \Delta_k\, w^k\, \mathrm{e}^{\mathrm{i}k\theta},$$

while for $\boldsymbol{w} \in \boldsymbol{H}(\mathrm{div};\Omega)$, resp. $\boldsymbol{H}(\mathbf{curl};\Omega)$:

$$\operatorname{div}\boldsymbol{w} = \frac{1}{\sqrt{2\pi}} \sum_{k\in\mathbb{Z}} \operatorname{div}_k \boldsymbol{w}^k \,\mathrm{e}^{\mathrm{i}k\theta}, \quad \text{resp.} \quad \mathbf{curl}\,\boldsymbol{w} = \frac{1}{\sqrt{2\pi}} \sum_{k\in\mathbb{Z}} \mathbf{curl}_k \boldsymbol{w}^k \,\mathrm{e}^{\mathrm{i}k\theta}.$$

Above, the operators for the mode k are defined as:

$$\mathbf{grad}_k\, w := \frac{\partial w}{\partial r}\,\mathbf{e}_r + \frac{\mathrm{i}k}{r}\,w\,\mathbf{e}_\theta + \frac{\partial w}{\partial z}\,\mathbf{e}_z\,; \qquad \Delta_k\, w := \frac{1}{r}\frac{\partial}{\partial r}\left(r\,\frac{\partial w}{\partial r}\right) - \frac{k^2}{r^2}\,w + \frac{\partial^2 w}{\partial z^2}\,;$$

$$\operatorname{div}_k \boldsymbol{w} := \frac{1}{r}\,\frac{\partial(r\,w_r)}{\partial r} + \frac{\mathrm{i}k}{r}\,w_\theta + \frac{\partial w_z}{\partial z}\,; \qquad (\mathbf{curl}_k\,\boldsymbol{w})_r := \frac{\mathrm{i}k}{r}\,w_z - \frac{\partial w_\theta}{\partial z}\,;$$

$$(\mathbf{curl}_k\,\boldsymbol{w})_\theta := \frac{\partial w_r}{\partial z} - \frac{\partial w_z}{\partial r}\,; \qquad (\mathbf{curl}_k\,\boldsymbol{w})_z := \frac{1}{r}\left(\frac{\partial(r\,w_\theta)}{\partial r} - \mathrm{i}k\,w_r\right).$$

As an immediate consequence, we have the following characterisation.

Proposition 2.8. *Let $\boldsymbol{X}_{(k)}(\omega)$ be the space*

$$\boldsymbol{X}_{(k)}(\omega) := \left\{\boldsymbol{v} \in \boldsymbol{L}^2_1(\omega) : \mathbf{curl}_k\,\boldsymbol{v} \in \boldsymbol{L}^2_1(\omega) \text{ and } \operatorname{div}_k \boldsymbol{v} \in L^2_1(\omega) \text{ and } \boldsymbol{v}\times\boldsymbol{n}|_{\gamma_b} = 0\right\},$$

endowed with the canonical norm $\|\boldsymbol{v}\|^2_{\boldsymbol{X},(k)} := \|\,\mathbf{curl}_k\,\boldsymbol{v}\|^2_{0,1} + \|\operatorname{div}_k \boldsymbol{v}\|^2_{0,1}$.

The field $\boldsymbol{u}$ belongs to $\boldsymbol{X}(\Omega)$ iff, for all $k \in \mathbb{Z}$, its Fourier coefficients $\boldsymbol{u}^k \in \boldsymbol{X}_{(k)}(\omega)$, and the sum $\sum_{k\in\mathbb{Z}} \|\boldsymbol{u}^k\|^2_{\boldsymbol{X},(k)}$ is finite. In this case, it is equal to $\|\boldsymbol{u}\|^2_{\boldsymbol{X}}$. A similar result holds for the magnetic boundary condition.

These spaces enjoy an important property.

Proposition 2.9. *The space $\boldsymbol{X}_{(k)}(\omega)$ is independent of k, for $|k| \geq 2$.*

Proof. In the seminal work by Birman and Solomyak [13], the following result is proved. Any field $\boldsymbol{u} \in \boldsymbol{X}(\Omega)$ can be decomposed as:

$$\boldsymbol{u} = \boldsymbol{u}_{BS} - \mathbf{grad}\,\varphi, \quad \text{where:} \tag{2.22}$$

$$\boldsymbol{u}_{BS} \in \boldsymbol{X}^{\mathrm{reg}}(\Omega) := \boldsymbol{X}(\Omega) \cap \boldsymbol{H}^1(\Omega), \tag{2.23}$$

$$\varphi \in \Phi(\Omega) := \left\{\varphi \in \overset{\circ}{H}{}^1(\Omega) : \Delta\varphi \in L^2(\Omega)\right\} \tag{2.24}$$

$$\text{and:} \quad \|\boldsymbol{u}_{BS}\|_1 + \|\varphi\|_1 + \|\Delta\varphi\|_0 \lesssim \|\boldsymbol{u}\|_{\boldsymbol{X}}\,. \tag{2.25}$$

Let us expand $\boldsymbol{u}$ in Fourier series: $\boldsymbol{u}(r,\theta,z) = \frac{1}{\sqrt{2\pi}} \sum_{k\in\mathbb{Z}} \boldsymbol{u}^k(r,z)\,\mathrm{e}^{\mathrm{i}k\theta}$, and similarly for $\boldsymbol{u}_{BS}$ and φ. The decomposition of the operator **grad** on the spectral basis (see above) shows that, for each mode $k \in \mathbb{Z}$, the following splitting holds:

$$\boldsymbol{u}^k = \boldsymbol{u}^k_{BS} - \mathbf{grad}_k\,\varphi^k = \boldsymbol{u}^k_{BS} - (\mathrm{i}k/r)\,\varphi^k\,\mathbf{e}_\theta - \mathbf{grad}_0\,\varphi^k. \tag{2.26}$$

Furthermore, the decomposition of the Laplace operator, and Propositions 2.4, 2.6 and 2.8 imply the following regularity properties:

$$\boldsymbol{u}^k_{BS} \in \boldsymbol{X}^{\mathrm{reg}}_{(k)}(\omega) = \left\{\boldsymbol{u} \in \boldsymbol{H}^1_{(k)}(\omega) : \boldsymbol{u}\times\boldsymbol{n}|_{\gamma_b} = 0\right\}, \tag{2.27}$$

$$\varphi^k \in \Phi_{(k)}(\omega) = \left\{\varphi \in H^1_{(k)}(\omega) \cap \overset{\diamond}{H}{}^1_1(\omega) : \Delta_k\varphi \in L^2_1(\omega)\right\}; \tag{2.28}$$

By Proposition 2.6 we know that the space $\boldsymbol{H}^1_{(k)}(\omega)$, and hence $\boldsymbol{X}^{\mathrm{reg}}_{(k)}(\omega)$, is independent of k for $|k| \geq 2$. The same holds for $\Phi_{(k)}(\omega)$, as a consequence of [20, Thm 3.2]. This same theorem also shows that functions in $\Phi_{(k)}(\omega)$ are of V^2_1 regularity near the axis γ_a. Therefore, $(\mathrm{i}k/r)\,\varphi^k$ is locally of V^1_1 regularity. Elsewhere, this function is of H^1 regularity and vanishes on γ_b. All together, we see that the vector field $(\mathrm{i}k/r)\,\varphi^k\,\mathbf{e}_\theta$ belongs to the regular space $\boldsymbol{X}^{\mathrm{reg}}_{(k)}(\omega)$. Thus, (2.26) shows that:

$$\forall k \in \mathbb{Z}, \quad \boldsymbol{u}^k \in \boldsymbol{X}^{\mathrm{reg}}_{(k)}(\omega) + \mathbf{grad}_0\,\Phi_{(k)}(\omega).$$

Assume for the moment that $\boldsymbol{u}$ has a single Fourier mode, i.e., let $\boldsymbol{u}(r,\theta,z) = \frac{1}{\sqrt{2\pi}}\,\boldsymbol{u}^{k_0}(r,z)\,\mathrm{e}^{\mathrm{i}k_0\theta}$, for any $\boldsymbol{u}^{k_0} \in \boldsymbol{X}_{(k_0)}(\omega)$. Setting $k = k_0$ in the above statement, we see that $\boldsymbol{X}_{(k_0)}(\omega) \subset \boldsymbol{X}^{\mathrm{reg}}_{(k_0)}(\omega) + \mathbf{grad}_0\,\Phi_{(k_0)}(\omega)$. The converse inclusion is proved by a similar argument. Finally, $\boldsymbol{X}_{(k_0)}(\omega) = \boldsymbol{X}^{\mathrm{reg}}_{(k_0)}(\omega) + \mathbf{grad}_0\,\Phi_{(k_0)}(\omega)$, which is independent of k_0 for $|k_0| \geq 2$.

Finally, we prove that the decomposition is continuous. With the equivalence of norms statements in Propositions 2.6 and 2.8, the bound (2.25) becomes:

$$\sum_{k\in\mathbb{Z}} \|\boldsymbol{u}^k_{BS}\|^2_{1,(k)} + \|\varphi^k\|^2_{1,(k)} + \|\Delta_k\varphi^k\|^2_{0,1} \lesssim \|\boldsymbol{u}^{k_0}\|^2_{\boldsymbol{X},(k_0)}.$$

On the left-hand side, the contribution of the mode k_0 is, of course, less than the sum. Evidently, it is possible to replace all others coefficients $\boldsymbol{u}^k_{BS}$ and φ^k with 0 without changing the value of $\boldsymbol{u}^{k_0} = \boldsymbol{u}^{k_0}_{BS} - \mathbf{grad}_{k_0}\,\varphi^{k_0}$. Substituting the symbol k for k_0, we finally obtain:

$$\|\boldsymbol{u}^k_{BS}\|_{1,(k)} + \|\varphi^k\|_{1,(k)} + \|\Delta_k\varphi^k\|_{0,1} \lesssim \|\boldsymbol{u}^k\|_{\boldsymbol{X},(k)}\,, \tag{2.29}$$

for any $\boldsymbol{u}^k \in \boldsymbol{X}_{(k)}(\omega)$. Moreover, the linearity of the differential operators and their decomposition on the spectral basis imply that (2.26)–(2.29) hold for all Fourier coefficients of all $\boldsymbol{u} \in \boldsymbol{X}(\Omega)$. □

Combining the decomposition (2.26) with the description of primal singularities of the Laplacian Δ_k in [12, §II.4], one characterises the regularity of these spaces in the Sobolev scale.

Theorem 2.10. *The following statements hold true. (See Figure 1 and Eq.* (2.1) *for the meaning of α_e and ν_c.)*

1. *The elements of $\boldsymbol{X}_{(k)}(\omega)$ are locally regular, i.e. $\boldsymbol{H}^1_{(k)}$, except in the neighbourhood of the reentrant edges and, for $k = 0$, of the sharp vertices.*
2. *The space $\boldsymbol{X}_{(0)}(\omega)$ is continuously embedded in $\boldsymbol{H}^s_{(0)}(\omega)$ for $s < s_M :=$* $\min\{\alpha_e : \boldsymbol{e}$ *reentrant edge* ; $\nu_c + \frac{1}{2} : \boldsymbol{c}$ *sharp vertex*$\}$.
3. *The space $\boldsymbol{X}_{(k)}(\omega)$, $|k| \geq 1$ is continuously embedded in $\boldsymbol{H}^s_{(k)}(\omega)$ for $s <$* $\alpha_{\min} := \min\{\alpha_e : \boldsymbol{e}$ *reentrant edge*$\}$.
4. *Consequently, $\boldsymbol{X}(\Omega)$ is continuously embedded in $\boldsymbol{H}^s(\Omega)$ for $s < s_M$. The bound is sharp.*

The Birman–Solomyak decomposition also holds with the magnetic boundary condition. In this case, there are no singularities in the vicinity of conical vertices, whatever their aperture [3, 30]; hence, the space is continuously embedded in $\boldsymbol{H}^s(\Omega)$ for $s < \alpha_{\min}$.

2.5. **Dimension reduction.** The linearity of Equations (2.15) or (2.16,2.17), together with the orthogonality of the different Fourier modes in $\boldsymbol{L}^2(\Omega)$, implies that the Fourier coefficients $(\boldsymbol{E}^k, \boldsymbol{B}^k)$ of $\boldsymbol{E}$ and $\boldsymbol{B}$ are solutions to similar formulations, with the operators $\mathbf{curl}_k$ and div_k. Namely, let us define:

$$a_k(\boldsymbol{u}, \boldsymbol{v}) = (\mathbf{curl}_k\, \boldsymbol{u} \mid \mathbf{curl}_k\, \boldsymbol{v}) + (\mathrm{div}_k\, \boldsymbol{u} \mid \mathrm{div}_k\, \boldsymbol{v})\,; \qquad (2.30)$$
$$b_k(\boldsymbol{v}, q) = (\mathrm{div}_k\, \boldsymbol{v} \mid q).$$

Then, we have the augmented formulation:
Find $\boldsymbol{E}^k \in \boldsymbol{X}_{(k)}(\omega)$ *such that, for all* $\boldsymbol{F} \in \boldsymbol{X}_{(k)}(\omega)$*:*

$$\frac{d^2}{dt^2}(\boldsymbol{E}^k(t) \mid \boldsymbol{F}) + a_k(\boldsymbol{E}^k(t), \boldsymbol{F}) = (\boldsymbol{\psi}^k(t) \mid \boldsymbol{F}). \qquad (2.31)$$

And the mixed augmented formulation writes:
Find $(\boldsymbol{E}^k, P^k) \in \boldsymbol{X}_{(k)}(\omega) \times L^2_1(\omega)$ *such that, for all* $(\boldsymbol{F}, q) \in \boldsymbol{X}_{(k)}(\omega) \times L^2_1(\omega)$*:*

$$\frac{d^2}{dt^2}(\boldsymbol{E}^k(t) \mid \boldsymbol{F}) + a_k(\boldsymbol{E}^k(t), \boldsymbol{F}) + b_k(\boldsymbol{F}, P^k(t)) = (\boldsymbol{\psi}^k(t) \mid \boldsymbol{F}), \qquad (2.32)$$
$$b_k(\boldsymbol{E}^k(t), q) = (\varrho^k(t) \mid q). \qquad (2.33)$$

Remark 2.11. Alternatively, the function $(r, \theta, z) \mapsto \boldsymbol{E}^k(r, z)\, \mathrm{e}^{\mathrm{i}k\theta}$ (defined in Ω) appears as the solution to (2.9) with single-mode sources $\boldsymbol{J}^k(r, z)\, \mathrm{e}^{\mathrm{i}k\theta}$ and $\varrho^k(r, z)\, \mathrm{e}^{\mathrm{i}k\theta}$. The same holds for $(r, \theta, z) \mapsto (\boldsymbol{E}^k(r, z)\, \mathrm{e}^{\mathrm{i}k\theta}, P^k(r, z)\, \mathrm{e}^{\mathrm{i}k\theta})$ as a solution to (2.11,2.12). This allows to transpose directly many known results from the three-dimensional framework to that of the weighted spaces adapted to each mode.

3. Analysis of the truncation error of the Fourier expansion

In order to evaluate this error, we introduce (as usual) the following scales of anisotropic Sobolev spaces.

Definition 3.1. Let $W(\Omega)$ be any Hilbert space of functions defined in Ω, and $s \geq 0$. The space $H^{s,W}(\Omega)$ is defined:

- when s is an integer, as the space of functions in $W(\Omega)$ such that *all their partial derivatives in* θ, up to order s, belong to $W(\Omega)$;
- otherwise, by appropriate interpolation between $H^{\lfloor s \rfloor, W}(\Omega)$ and $H^{\lfloor s \rfloor + 1, W}(\Omega)$.

In both cases, $H^{s,W}(\Omega)$ is a Hilbert space for its canonical norm. For the sake of simplicity, we shall denote $H^{m,s}(\Omega) := H^{s,H^m}(\Omega)$ and $\boldsymbol{H}^{m,s}(\Omega) := H^{s,\boldsymbol{H}^m}(\Omega)$ when $W(\Omega) = H^m(\Omega)$ or $\boldsymbol{H}^m(\Omega)$.

In order to describe this regularity in spectral terms, we assume from now on that $W(\Omega)$ fulfils either one of the following properties.

- Either, $W(\Omega)$ is continuously embedded in $L^2(\Omega)^d$, $d \in \{1, 3\}$. Then, the Fourier coefficients $(w^k)_{k\in\mathbb{Z}}$ of $w \in W(\Omega)$ are defined in the usual way. Let $(W_{(k)}(\omega))_{k\in\mathbb{Z}}$ be the spaces of such coefficients; their norms can be chosen such as to have: $\|w\|^2_{W(\Omega)} \approx \sum_{k\in\mathbb{Z}} \|w^k\|^2_{W_{(k)}(\omega)}$.
- Or, $W(\Omega)$ is the dual space of a space $V(\Omega)$, itself continuously and densely embedded in $L^2(\Omega)^d$, seen as the pivot space. Then, the $(w^k)_{k\in\mathbb{Z}}$ are defined by duality. The spaces $W_{(k)}(\omega)$ which they span appear as the duals of the subspaces $V_{(k)}(\omega)$ of $L^2_1(\omega)^d$. If the $(V_{(k)}(\omega))_{k\in\mathbb{Z}}$ satisfy an equivalence of norms result as above, so do the $(W_{(k)}(\omega))_{k\in\mathbb{Z}}$.

Then, it is standard matter to check (see e.g. [16, Thm 1.1]) the following result.

Lemma 3.2. *Let $W(\Omega)$ and $(W_{(k)}(\omega))_{k\in\mathbb{Z}}$ as in one of the two above cases, and $s \geq 0$. The following equivalence of norms holds:*

$$\forall w \in H^{s,W}(\Omega), \quad \|w\|^2_{H^{s,W}(\Omega)} \approx \sum_{k\in\mathbb{Z}}(1+|k|^{2s})\,\|w^k\|^2_{W_{(k)}(\omega)}, \tag{3.1}$$

from which one deduces the truncation estimate

$$\forall w \in H^{s,W}(\Omega),\ \forall N \geq 1, \quad \left\|w - w^{[N]}\right\|^2_{W(\Omega)} \lesssim N^{-2s}\,\|w\|^2_{H^{s,W}(\Omega)}, \tag{3.2}$$

for the truncated Fourier expansion $w^{[N]}$ defined in (2.20).

The next Proposition is an immediate consequence of Lemma 3.2.

Proposition 3.3. *Assume that the electric field has the regularity $\boldsymbol{E} \in \mathcal{C}^0(0,T;H^{\sigma,\boldsymbol{X}}(\Omega)) \cap \mathcal{C}^1(0,T;\boldsymbol{H}^{0,\sigma}(\Omega))$, for some $\sigma \geq 0$. There holds:*

$$\begin{aligned} \forall t \in [0,T], \quad & \|\dot{\boldsymbol{E}}^{[N]}(t) - \dot{\boldsymbol{E}}(t)\|_0^2 + \|\boldsymbol{E}^{[N]}(t) - \boldsymbol{E}(t)\|^2_{\boldsymbol{X}} \lesssim \\ & N^{-2\sigma}\left\{\|\dot{\boldsymbol{E}}(t)\|^2_{\boldsymbol{H}^{0,\sigma}(\Omega)} + \|\boldsymbol{E}(t)\|^2_{H^{\sigma,\boldsymbol{X}}(\Omega)}\right\}, \end{aligned} \tag{3.3}$$

for any fixed integer $N \geq 2$.

Above, the notation $\dot{\boldsymbol{E}}$ is simply $\partial_t \boldsymbol{E}$. It is worth noting that such a regularity in θ for the solution to Maxwell's equations can follow from a similar regularity assumption for the data: roughly speaking, the direction θ is orthogonal to the singularities and "it does not see them".

Proposition 3.4. *Assume that, for some $m \in \mathbb{N}$ and $\sigma > 0$, the data satisfy $\boldsymbol{J} \in H^{m+1}(0,T;\boldsymbol{H}^{0,\sigma}(\Omega))$, $\varrho \in H^m(0,T;\overset{\circ}{H}{}^{1,\sigma}(\Omega))$ in the augmented formulation, $\varrho \in \mathcal{C}^m(0,T;H^{0,\sigma}(\Omega)) \cap H^{m+2}(0,T;H^{-1,\sigma}(\Omega))$ in the mixed augmented formulation. Then, the electric field has the regularity $\mathcal{C}^m(0,T;H^{\sigma,\boldsymbol{X}}(\Omega)) \cap \mathcal{C}^{m+1}(0,T;\boldsymbol{H}^{0,\sigma}(\Omega))$, with continuous dependence.*

Proof. We examine the case $m = 0$; the general case can be deduced by combining the following ideas with those of Proposition 2.3. By Remark 2.11, we can write the continuity estimate for the solution to (2.31):

$$\|\dot{\boldsymbol{E}}^k(t)\|^2_{0,1} + \|\boldsymbol{E}^k(t)\|^2_{\boldsymbol{X},(k)} \lesssim \|\boldsymbol{\psi}^k\|^2_{L^2(0,t;\boldsymbol{L}^2_1(\omega))} \lesssim \|\boldsymbol{J}^k\|^2_{H^1(0,t;\boldsymbol{L}^2_1(\omega))} + \|\varrho^k\|^2_{L^2(0,t;\overset{\circ}{H}{}^1_{(k)}(\omega))}.$$

Then, we multiply this bound by $(1+|k|^{2\sigma})$, and add the bounds for the values $k = -N$ to N:

$$\begin{aligned} & \sum_{k=-N}^{N}(1+|k|^{2\sigma})\left\{\|\dot{\boldsymbol{E}}^k(t)\|^2_{0,1} + \|\boldsymbol{E}^k(t)\|^2_{\boldsymbol{X},(k)}\right\} \\ & \qquad \lesssim \sum_{k=-N}^{N}(1+|k|^{2\sigma})\left\{\|\boldsymbol{J}^k\|^2_{H^1(0,t;\boldsymbol{L}^2_1(\omega))} + \|\varrho^k\|^2_{L^2(0,t;\overset{\circ}{H}{}^1_{(k)}(\omega))}\right\} \end{aligned}$$

If $\boldsymbol{J} \in H^1(0,t;\boldsymbol{H}^{0,\sigma}(\Omega))$ and $\varrho \in L^2(0,t;\overset{\circ}{H}{}^{1,\sigma}(\Omega))$, then the right-hand side is bounded by the squared norms of $\boldsymbol{J}$ and ϱ in these spaces when $N \to \infty$, according to Lemma 3.2. Thus, the same Lemma implies that $\dot{\boldsymbol{E}}(t) \in \boldsymbol{H}^{0,\sigma}(\Omega)$ and $\boldsymbol{E}(t) \in H^{\sigma,\boldsymbol{X}}(\Omega)$, and that their squared norms are controlled by the aforementioned squared norms of $\boldsymbol{J}$ and ϱ. Of course, the same reasoning holds for the solution to (2.32,2.33). □

Before ending this section, it must be observed that in many practical situations the Fourier coefficients ϱ^k and $\boldsymbol{J}^k$ cannot be computed exactly. So they have to be approximated by quadrature formulas. Introducing the nodes $\theta_m := 2m\pi/(2N+1)$, for $-N \le m \le N$, we define the approximate Fourier coefficients and approximate truncated expansion of the function w by the formulas:

$$w_\star^k(r,z) \quad := \quad \frac{\sqrt{2\pi}}{2N+1} \sum_{m=-N}^{N} w(r,\theta_m,z)\, \mathrm{e}^{-\mathrm{i}k\theta_m}\,; \tag{3.4}$$

$$w_\star^{[N]}(r,\theta,z) \quad := \quad \frac{1}{\sqrt{2\pi}} \sum_{k=-N}^{N} w_\star^k(r,z)\, \mathrm{e}^{\mathrm{i}k\theta}. \tag{3.5}$$

These approximate coefficients are the same as in [12, 11, 9]; however, we shall need slightly more general approximation estimates than in those References.

Proposition 3.5. *Let $s > t \ge 0$ such that $s - t > \frac{1}{2}$. The following estimates hold for all $w \in H^{s,W}(\Omega)$:*

$$\|w_\star^{[N]} - w^{[N]}\|^2_{W(\Omega)} \quad \lesssim \quad N^{-2s}\, \|w\|^2_{H^{s,W}(\Omega)}\,; \tag{3.6}$$

$$\sum_{k=-N}^{N} (1+|k|^{2t})\, \|w^k - w_\star^k\|^2_{W_{(k)}(\omega)} \quad \lesssim \quad N^{-2(s-t)}\, \|w\|^2_{H^{s,W}(\Omega)}. \tag{3.7}$$

Proof. The first estimate is a particular case of the second; both rely on the identity [16]: $w_\star^k = \sum_{\ell\in\mathbb{Z}} w^{k+(2N+1)\,\ell}$. One can easily adapt the proof of [12, Proposition VI.4.1], remarking that only regularity in θ is involved; see also [16, Thm 1.2]. $\square$

The linearity of Maxwell's equations and the previous Proposition imply the following results.

Proposition 3.6. *Let $\varrho_\star^k(t)$, $\boldsymbol{J}_\star^k(t)$, $\boldsymbol{E}_\star^k(t)$, $P_\star^k(t)$ and $\varrho_\star^{[N]}(t)$, $\boldsymbol{J}_\star^{[N]}(t)$, $\boldsymbol{E}_\star^{[N]}(t)$, $P_\star^{[N]}(t)$ be defined as in* (3.4) *and* (3.5)*, at each instant t.*

1. *$\boldsymbol{E}_\star^k$, respectively $(\boldsymbol{E}_\star^k, P_\star^k)$, is the solution to* (2.31)*, resp.* (2.32)–(2.33)*, with data $(\varrho^k, \boldsymbol{J}^k)$ replaced with $(\varrho_\star^k, \boldsymbol{J}_\star^k)$.*
2. *$\boldsymbol{E}_\star^{[N]}$, respectively $(\boldsymbol{E}_\star^{[N]}, P_\star^{[N]})$ is the solution to* (2.15)*, resp.* (2.16)–(2.17)*, with data $(\varrho, \boldsymbol{J})$ replaced with $(\varrho_\star^{[N]}, \boldsymbol{J}_\star^{[N]})$.*
3. *Assuming $\boldsymbol{E} \in \mathcal{C}^0(0,T; H^{\sigma,\boldsymbol{X}}(\Omega)) \cap \mathcal{C}^1(0,T; \boldsymbol{H}^{0,\sigma}(\Omega))$, for some $\sigma > \frac{1}{2}$, we have:*

$$\forall t \in [0,T], \quad \|\dot{\boldsymbol{E}}^{[N]}(t) - \dot{\boldsymbol{E}}_\star^{[N]}(t)\|_0^2 + \|\boldsymbol{E}^{[N]}(t) - \boldsymbol{E}_\star^{[N]}(t)\|^2_{\boldsymbol{X}} \lesssim \\ N^{-2\sigma} \left\{ \|\dot{\boldsymbol{E}}(t)\|^2_{\boldsymbol{H}^{0,\sigma}(\Omega)} + \|\boldsymbol{E}(t)\|^2_{H^{\sigma,\boldsymbol{X}}(\Omega)} \right\}. \tag{3.8}$$

In the following Section, we shall examine the discretisation of the variational formulations (2.31) and (2.32,2.33), with data $(\varrho_\star^k, \boldsymbol{J}_\star^k)$.

4. Discretisations and abstract approximation results

4.1. **General framework.** The discretisation of the variational formulations for each mode k, viz. (2.31) or (2.32,2.33) will follow the usual principles. We suppose that we are given a family of regular triangulations $(\mathcal{T}_h)_{h>0}$ of the meridian domain ω. The space of electric fields $\boldsymbol{X}_{(k)}(\omega)$ will be approached by nodal elements, complemented by singular functions in the case of the SCM. Thus, for the UNFEM we use:

$$\mathbb{X}^h_{(k)} = \mathbb{X}^{\mathrm{reg};h}_{(k)} := \left\{ \boldsymbol{v}_h \in \mathcal{C}^0(\overline{\omega})^3 \cap \boldsymbol{X}_{(k)}(\omega) : \boldsymbol{v}_{h|T} \in \mathbb{P}_\kappa(T)^3,\ \forall T \in \mathcal{T}_h \right\}, \tag{4.1}$$

($\kappa \geq 1$ is an integer and $\mathbb{P}_\kappa(T)$ denotes the set of polynomials of degree at most κ over T) seen as a subspace of $\boldsymbol{X}_{(k)}(\omega)$. Whereas, for the SCM, we use the space

$$\mathbb{X}^h_{(k)} = \mathbb{X}^{\mathrm{reg};h}_{(k)} \oplus \mathbb{X}^{\mathrm{sing};h}_{(k)}, \tag{4.2}$$

where the *singular complement* $\mathbb{X}^{\mathrm{sing};h}_{(k)}$ will be described in §§5.1 and 6.1.

The multiplier space $Q = L^2_1(\omega)$ of the mixed formulation will be approached by the space Q_h, which will also be generated by nodal finite elements. We will always choose the couple $(\mathbb{X}^h_{(k)}, Q_h)$ such as to satisfy the two usual requirements, namely, the ellipticity of a_k on the discrete kernel of b_k, and a uniform (with respect to h) discrete inf-sup condition. For the UNFEM and SCM, one can use $Q_h = P_{\kappa-1,h}$, the space of $\mathbb{P}_{\kappa-1}$ finite elements seen as a subspace of $L^2(\Omega)$. This amounts to using the well-known $\mathbb{P}_\kappa - \mathbb{P}_{\kappa-1}$ Taylor–Hood finite element [31, pp. 176 ff.].

As for the time discretisation, we shall concentrate upon a totally implicit scheme which is inconditionally stable [21]. An explicit variant will be briefly discussed at the end of §6. The time mesh being defined by the instants $t^n = n\,\tau$, the value of the field $\boldsymbol{u}$ at time t^n is denoted $\boldsymbol{u}^n$; for its k-th Fourier coefficient $\boldsymbol{u}^k$, we shall write $\boldsymbol{u}^{k;n}$. If this field is defined in continuous time, its successive time derivatives are denoted $\dot{\boldsymbol{u}}^{k;n} = \partial_t \boldsymbol{u}^k(t^n)$, $\ddot{\boldsymbol{u}}^{k;n} = \partial_t^2 \boldsymbol{u}^k(t^n)$, etc. The discrete time derivatives of the field $\boldsymbol{u}^k$ are given by: $\partial_\tau \boldsymbol{u}^{k;n} := \tau^{-1}\,(\boldsymbol{u}^{k;n} - \boldsymbol{u}^{k;n-1})$, or $\partial_{2\tau} \boldsymbol{u}^{k;n} := (2\tau)^{-1}\,(\boldsymbol{u}^{k;n} - \boldsymbol{u}^{k;n-2})$.

4.2. **Fully discrete formulations.** For the augmented formulations, the totally implicit scheme writes:
Find $\boldsymbol{E}_h^{k;n+1} \in \mathbb{X}^h_{(k)}$ *such that, for all* $\boldsymbol{F}_h \in \mathbb{X}^h_{(k)}$,

$$\begin{aligned}(\partial_\tau^2 \boldsymbol{E}_h^{k;n+1} \mid \boldsymbol{F}_h) + a_k(\boldsymbol{E}_h^{k;n+1}, \boldsymbol{F}_h) \\ = -(\partial_\tau \boldsymbol{J}_\star^{k;n+1} \mid \boldsymbol{F}_h) + (\varrho_\star^{k;n+1} \mid \operatorname{div} \boldsymbol{F}_h)\,;\end{aligned} \tag{4.3}$$

This equation must be supplemented with initial conditions; so one sets:

$$\boldsymbol{E}_h^{k;0} = \boldsymbol{\Pi}_h \boldsymbol{E}_0^k, \quad \boldsymbol{E}_h^{k;1} \text{ solution to:} \tag{4.4}$$

$$\begin{aligned}\tau^{-2}\,(\boldsymbol{E}_h^{k;1} - \boldsymbol{E}_h^{k;0} - \tau\,\boldsymbol{\Pi}_h \boldsymbol{E}_1^k \mid \boldsymbol{F}_h) + a_k(\boldsymbol{E}_h^{k;1} - \tfrac{1}{2}\,\boldsymbol{E}_h^{k;0}, \boldsymbol{F}_h) \\ = -(\partial_\tau \boldsymbol{J}_\star^{k;1} - \tfrac{1}{2}\partial_\tau \boldsymbol{J}_\star^{k;0} \mid \boldsymbol{F}_h) + (\varrho_\star^{k;1} - \tfrac{1}{2}\varrho_\star^{k;0} \mid \operatorname{div} \boldsymbol{F}_h)\,.\end{aligned} \tag{4.5}$$

The operator $\boldsymbol{\Pi}_h$ is an interpolation/projection operator which depends on the numerical method.

As a natural extension, we have the mixed augmented formulation:
Find $(\boldsymbol{E}_h^{k;n+1}, P_h^{k;n+1}) \in \mathbb{X}^h_{(k)} \times Q_h$ *such that, for all* $(\boldsymbol{F}_h, q_h) \in \mathbb{X}^h_{(k)} \times Q_h$,

$$\begin{aligned}(\partial_\tau^2 \boldsymbol{E}_h^{k;n+1} \mid \boldsymbol{F}_h) + a_k(\boldsymbol{E}_h^{k;n+1}, \boldsymbol{F}_h) + b_k(\boldsymbol{F}_h, P_h^{k;n+1}) \\ = -(\partial_\tau \boldsymbol{J}_\star^{k;n+1} \mid \boldsymbol{F}_h) + (\varrho_\star^{k;n+1} \mid \operatorname{div} \boldsymbol{F}_h)\,;\end{aligned} \tag{4.6}$$

$$b_k(\boldsymbol{E}_h^{k;n+1}, q_h) = (\varrho_\star^{k;n+1} \mid q_h). \tag{4.7}$$

4.3. **Mode-wise estimates.** To obtain such estimates, we suppose that there exists a subspace $\boldsymbol{X}^s(\Omega) \subset \boldsymbol{X}(\Omega)$, to which the solution to Maxwell's equation belongs provided the data are regular enough, and such that its spaces of Fourier coefficients $\boldsymbol{X}^s_{(k)}(\omega)$ satisfy an approximation inequality of the form:

$$\forall \boldsymbol{u} \in \boldsymbol{X}^s_{(k)}(\omega),\ \exists \boldsymbol{u}_h \in \mathbb{X}^h_{(k)},\ \|\boldsymbol{u} - \boldsymbol{u}_h\|_{\boldsymbol{X},(k)} \lesssim \epsilon(s,h,k)\, \|\boldsymbol{u}\|_{\boldsymbol{X},s,(k)}. \tag{4.8}$$

Moreover, the anisotropic Sobolev space $H^{\sigma,\boldsymbol{X}^s}(\Omega)$ will be denoted $\boldsymbol{X}^{s,\sigma}(\Omega)$, for the sake of simplicity. The construction of this space and the establishment of the approximation inequality will be carried out in §§5 and 6. For the moment, we assume that the data and the solution are regular enough, typically $\boldsymbol{E} \in H^2(-\delta,T;\boldsymbol{X}^{s,q+\sigma}(\Omega)) \cap H^3(-\delta,T;\boldsymbol{H}^{0,\sigma}(\Omega))$ and $\boldsymbol{J} \in H^2(-\delta,T;\boldsymbol{H}^{0,\sigma}(\Omega))$, where $\sigma > \frac{1}{2}$ and $q \in [1,2]$, and δ is a small multiple of the time step τ. The relevance of these conditions will be examined in §6.3 below.

Proposition 4.1. *Let* $\left(\boldsymbol{E}_h^{k;n}\right)_n$ *be the solution to the discrete formulation* (4.3). *The following error estimates hold:*

$$\|\partial_\tau \boldsymbol{E}_h^{k;n} - \dot{\boldsymbol{E}}_\star^{k;n}\|_{0,1}^2 + \|\boldsymbol{E}_h^{k;n} - \boldsymbol{E}_\star^{k;n}\|_{\boldsymbol{X},(k)}^2 \lesssim\ m(s,h,k)\,, \tag{4.9}$$

$$\|\boldsymbol{E}_h^{k;n} - \boldsymbol{E}_\star^{k;n}\|_{0,1}^2 \lesssim\ m(s,h,k)\,, \tag{4.10}$$

where $m(s,h,k) := \epsilon(s,h,k)^2\, \|\boldsymbol{E}_\star^k\|^2_{H^2(\boldsymbol{X}^s_{(k)}(\omega))}$

$$+ \tau^2 \left[\|\boldsymbol{E}_\star^k\|^2_{H^3(\boldsymbol{L}^2_1(\omega))} + \|\boldsymbol{J}_\star^k\|^2_{H^2(\boldsymbol{L}^2_1(\omega))}\right].$$

Proof. This follows, *mutatis mutandis*, from the estimates of [21, §5], thanks to the interpretation of (4.3) as the trace, in a meridian half-plane, of a 3D formulation in which the sources have only one Fourier mode. □

Now we examine the mixed augmented formulation, following the lines of [21, §7]. The usual difficulty in the numerical analysis of mixed problems is the derivation of a uniform (with respect to h) discrete inf-sup condition (DISC). Here, this issue is compounded by that of the dependence of this condition on the Fourier mode k. To our knowledge, no DISC *uniform in both h and k* has been yet derived for Maxwell or other mixed equations. So, we shall work with a (maybe not optimal) condition, which is uniform in h, but depends weakly on k.

Lemma 4.2. *For the $\mathbb{P}_2$–$\mathbb{P}_1$ Taylor–Hood element, there exists a constant β, independent of h and k, such that:*

$$\forall q_h \in Q_h, \qquad \sup_{\boldsymbol{v}_h \in \mathbb{X}^h_{(k)}} \frac{b_k(\boldsymbol{v}_h, q_h)}{\|\boldsymbol{v}_h\|_{\boldsymbol{X},(k)}} \geq \beta\,(1+|k|)^{-1}\, \|q_h\|_{0,1}\,. \tag{4.11}$$

Proof. In [9, Lemma 3.5], the following DISC is proven for the Stokes problem:

$$\forall q_h \in Q_{h(k)}, \qquad \sup_{\boldsymbol{v}_h \in \mathbb{H}^\diamond_{h(k)}} \frac{(\operatorname{div}_k \boldsymbol{v}_h \mid q_h)}{\|\boldsymbol{v}_h\|_{1,(k)}} \geq \tilde{\beta}\,(1+|k|)^{-1}\, \|q_h\|_{0,1}\,. \tag{4.12}$$

For $k \neq 0$, one has $Q_{h(k)} = Q_h$, whereas $Q_{h(0)} = \{q_h \in Q_h : \iint_\omega q_h\, r\,\mathrm{d}r\,\mathrm{d}z = 0\}$. Then $\mathbb{H}^\diamond_{h(k)}$ is

$$\mathbb{H}^\diamond_{h(k)} := \left\{\boldsymbol{w}_h \in \mathcal{C}^0(\overline{\omega})^3 \cap \mathring{\boldsymbol{H}}^1_{(k)}(\omega) : \boldsymbol{w}_h|_K \in \mathbb{P}_2(K)^3,\ \forall K \in \mathcal{T}_h\right\},$$

thus, it is a subspace of our $\mathbb{X}^h_{(k)}$. According for instance to [1, Rmk 2.6], there holds $|\boldsymbol{w}|_1 = \|\boldsymbol{w}\|_{\boldsymbol{X}}$, for all $\boldsymbol{w} \in \overset{\circ}{\boldsymbol{H}}{}^1(\Omega)$, and it follows that $\|\boldsymbol{w}\|_{1,(k)} = \|\boldsymbol{w}\|_{\boldsymbol{X},(k)}$ for $\boldsymbol{w} \in \overset{\circ}{\boldsymbol{H}}{}^1_{(k)}(\Omega)$. So, one can replace the norm $\|\boldsymbol{v}_h\|_{1,(k)}$ with $\|\boldsymbol{v}_h\|_{\boldsymbol{X},(k)}$ in (4.12), for all $\boldsymbol{v}_h \in \mathbb{H}^\diamond_{h(k)}$. For $k \neq 0$, this implies (4.11) since the supremum is greater on the bigger space $\mathbb{X}^h_{(k)}$.

For $k = 0$, one has to deal with discrete Lagrange multipliers whose mean value over Ω is not 0 (recall that $Q_h = Q_{h(0)} \oplus \mathbb{R}$). This difficulty can be overcome by using an *ad hoc* discrete field of $\mathbb{X}^h_{(0)}$ to provide a lower bound in (4.11) for $q_h = 1$. A similar result has been already obtained in [18, pp. 830–831] in an unweighted framework, and its proof can be easily adapted to our case. Let us sketch briefly how it is obtained. Consider γ', a side of γ_b that does not include any conical vertex. One checks easily that there exists $v' \in \mathcal{C}^2(\overline{\omega})$ such that: the support of $v'_{|\partial\omega}$ is a compact subset of γ'; the support of v' is included in $\{(r,z)\ :\ r \geq r_0\}$ for some $r_0 > 0$; last, $\int_{\gamma'} v' r\,\mathrm{d}r = 1$. Defining $\boldsymbol{v'} = v'\,\boldsymbol{n}_{|\gamma'}$, one has $\boldsymbol{v'} \in \mathcal{C}^2(\overline{\omega})^2$ and $(\mathrm{div}_0\,\boldsymbol{v'} \mid 1) = 1$.

Then, one builds a suitable approximation v'_h of v', and $\boldsymbol{v}'_h = v'_h\,\boldsymbol{n}_{|\gamma'}$, such that $(\mathrm{div}_0\,\boldsymbol{v}'_h \mid 1) = 1$. Thanks to the smoothness of v', one has $\|\boldsymbol{v}'_h\|_{\boldsymbol{X},(0)} \lesssim 1$. For $q_h \in \mathbb{R}$, one now derives the lower bound in (4.11) by choosing $\boldsymbol{v}'_h$ as the *ad hoc* test-field. Finally, given any $q_h \in Q_h$, let us split it as $q_h = q_{h(0)} + \overline{q}_h$, with $q_{h(0)} \in Q_{h(0)}$ and $\overline{q}_h \in \mathbb{R}$. One derives (4.11) by choosing $\boldsymbol{v}_h = \alpha\boldsymbol{v}_{h(0)} + \overline{q}_h\boldsymbol{v}'_h$, with $\boldsymbol{v}_{h(0)}$ a test-field achieving the condition for $q_{h(0)}$ (since we already know that (4.11) holds when q_h spans $Q_{h(0)}$), and $\alpha \in \mathbb{R}$. An *ad hoc* value of α is obtained by elementary computations (using for instance Young's inequality), leading to condition (4.11), for any $q_h \in Q_h$. □

With this result, we can derive two important properties. The first is the so-called *strong approximability* of the kernel of b_k; we recall that the continuous and discrete kernels are defined as:

$$\begin{aligned} \boldsymbol{K}_{(k)}(\omega) &:= \left\{\boldsymbol{v} \in \boldsymbol{X}_{(k)}(\omega) : b_k(\boldsymbol{v}, q) = 0,\ \forall q \in L^2_1(\omega)\right\}, \\ \mathbb{K}^h_{(k)} &:= \left\{\boldsymbol{v}_h \in \mathbb{X}^h_{(k)} : b_k(\boldsymbol{v}_h, q_h) = 0,\ \forall q_h \in Q_h\right\}. \end{aligned}$$

The second is the error estimate between the solution to the static mixed problem: *Given $\boldsymbol{f} \in \boldsymbol{X}_{(k)}(\omega)'$ and $g \in L^2_1(\omega)$, find $(\boldsymbol{u}, p) \in \boldsymbol{X}_{(k)}(\omega) \times L^2_1(\omega)$ such that, $\forall(\boldsymbol{v}, q) \in \boldsymbol{X}_{(k)}(\omega) \times L^2_1(\omega)$:*

$$a_k(\boldsymbol{u}, \boldsymbol{v}) + b_k(\boldsymbol{v}, p) = \langle \boldsymbol{f}, \boldsymbol{v}\rangle, \tag{4.13}$$

$$b_k(\boldsymbol{u}, q) = (g \mid q), \tag{4.14}$$

and that of its finite element discretisation, which writes:
Find $(\boldsymbol{u}_h, p_h) \in \mathbb{X}^h_{(k)} \times Q_h$ such that, $\forall(\boldsymbol{v}_h, q_h) \in \mathbb{X}^h_{(k)} \times Q_h$:

$$a_k(\boldsymbol{u}_h, \boldsymbol{v}_h) + b_k(\boldsymbol{v}_h, p_h) = \langle \boldsymbol{f}, \boldsymbol{v}_h\rangle, \tag{4.15}$$

$$b_k(\boldsymbol{u}_h, q_h) = (g \mid q_h). \tag{4.16}$$

Proposition 4.3. *The following approximation inequality holds:*
(4.17)

$$\forall \boldsymbol{u} \in \boldsymbol{K}_{(k)}(\omega) \cap \boldsymbol{X}^s_{(k)}(\omega),\ \exists \boldsymbol{u}_h \in \mathbb{K}^h_{(k)},\quad \|\boldsymbol{u}_h - \boldsymbol{u}\|_{\boldsymbol{X},(k)} \lesssim (1+|k|)\,\epsilon(s,h,k)\,\|\boldsymbol{u}\|_{\boldsymbol{X},s,(k)}.$$

Therefore, if the solution $(\boldsymbol{u}, p)$ *to* (4.13)–(4.14) *belongs to* $\boldsymbol{X}^s_{(k)}(\omega) \times H^1_1(\omega)$*, the following estimate holds:*

$$\|\boldsymbol{u}_h - \boldsymbol{u}\|_{\boldsymbol{X},(k)} + \|p_h - p\|_{0,1} \lesssim (1+|k|)\,\epsilon(s,h,k)\,\|\boldsymbol{u}\|_{\boldsymbol{X},s,(k)} + h\,\|p\|_{1,1}\,. \tag{4.18}$$

Proof. Use [31, Chapter II, Thm 1.1] and the previous lemma; the p part of the error is bounded using the weighted Clément operator of [8, §4.3]. ☐

The analysis of [21, §7] can be carried over to our case. Compared with their counterparts in that article, the error estimate (4.18) and the approximation inequality (4.17) contain a factor $1+|k|$ in front of $\epsilon(s,h,k)$. Also, it is better to use L^2_1 error estimates for (4.15,4.16) derived from the Weber inequality than derived from the Nitsche trick, which yields a bound in $(1+k^2)\,\epsilon(s,h,k)^2$. The term of higher power in h is of no use, being hidden by other terms with a smaller exponent; thus, the higher power in k appears unwelcome.

Proposition 4.4. *Let* $\left(\boldsymbol{E}^{k;n}_h, P^{k;n}_h\right)_n$ *be the solution to the discrete formulation* (4.6)–(4.7)*. The following error estimates hold:*

$$\|\partial_\tau \boldsymbol{E}^{k;n}_h - \dot{\boldsymbol{E}}^{k;n}_\star\|^2_{0,1} + \|\boldsymbol{E}^{k;n}_h - \boldsymbol{E}^{k;n}_\star\|^2_{\boldsymbol{X},(k)} \lesssim\ m'(s,h,k)\,, \tag{4.19}$$

$$\|\boldsymbol{E}^{k;n}_h - \boldsymbol{E}^{k;n}_\star\|^2_{0,1} \lesssim\ m'(s,h,k)\,, \tag{4.20}$$

where $m'(s,h,k) := (1+k^2)\,\epsilon(s,h,k)^2\,\|\boldsymbol{E}^k_\star\|^2_{H^2(\boldsymbol{X}^s_{(k)}(\omega))}$

$$+\ \tau^2\,\left[\|\boldsymbol{E}^k_\star\|^2_{H^3(\boldsymbol{L}^2_1(\omega))} + \|\boldsymbol{J}^k_\star\|^2_{H^2(\boldsymbol{L}^2_1(\omega))}\right].$$

5. Theoretical foundations of the SCM and FSCM

In this section, we describe the fields in $\boldsymbol{X}(\Omega)$ near the edges and vertices and study the regularising properties of the elliptic operators associated to the forms $a_k(\cdot,\cdot)$ and $a(\cdot,\cdot)$.

We use the notations of Figure 1: near any corner $\boldsymbol{j}$ of $\partial\omega$, we choose two neighbourhoods $\omega_j \subset\subset \omega'_j$ which stay away from the other corners and from the sides which do not contain $\boldsymbol{j}$. Local polar coordinates (ρ_j, ϕ_j) are used in ω'_j; we choose a cutoff function η_j, depending on ρ_j only, such that $\eta_j \equiv 1$ in ω_j and $\eta_j \equiv 0$ outside ω'_j. The symbol $\boldsymbol{j}$ will be replaced by $\boldsymbol{e}$ (resp. $\boldsymbol{c}$), when the corner is off-axis (resp. on the axis), i.e. it is the trace of a circular edge (resp. a conical vertex). For any off-axis corner $\boldsymbol{e}$, we denote $a_e = r(\boldsymbol{e})$ its distance to the z-axis, and ϕ^0_e the angle between the r-axis and the side $\phi_e = 0$. Near an on-axis corner $\boldsymbol{c}$, we always take $\phi_c = 0$ on the axis γ_a.

5.1. Description of singularities.

Let $\boldsymbol{u}$ be an arbitrary field in $\boldsymbol{X}(\Omega)$. We start from the Birman–Solomyak decomposition (2.26) at the mode k: $\boldsymbol{u}^k = \boldsymbol{u}^k_{BS} - \mathbf{grad}_k\,\varphi^k$, with $\boldsymbol{u}^k_{BS} \in \boldsymbol{X}^{\mathrm{reg}}_{(k)}(\omega)$, $\varphi^k \in \Phi_{(k)}(\omega)$, see (2.27), (2.28). We combine this with the regular-singular decomposition of the functions in $\Phi_{(k)}(\omega)$ from [12, §II.4]:

$$\varphi^0 = \varphi^0_* + \sum_{\text{r.e}} \lambda^e_0\, S^e_0 + \sum_{\text{s.v.}} \lambda^c_0\, S^c_0\,; \quad \varphi^k = \varphi^k_* + \sum_{\text{r.e}} \lambda^e_k\, S^e_k \quad \text{for } |k| \geq 1\,; \tag{5.1}$$

$$\text{with:}\quad \varphi^k_* \in H^2_{(k)}(\omega) \cap \overset{\diamond}{H}{}^1_1(\omega), \quad \forall k,$$

$$S^e_k(\rho_e, \phi_e) = \eta_e(\rho_e)\, \mathrm{e}^{-|k|\,\rho_e}\, \rho_e^{\alpha_e}\, \sin(\alpha_e \phi_e), \tag{5.2}$$

$$S^c_0(\rho_c, \phi_c) = \eta_c(\rho_c)\, \rho_c^{\nu_c}\, P_{\nu_c}(\cos\phi_c). \tag{5.3}$$

Thus we arrive at:

$$\boldsymbol{u}^0 = \boldsymbol{u}^0_* - \sum_{\text{r.e}} \lambda^e_0\, \mathbf{grad}_0\, S^e_0 - \sum_{\text{s.v.}} \lambda^c_0\, \mathbf{grad}_0\, S^c_0\,; \tag{5.4}$$

$$\boldsymbol{u}^k = \boldsymbol{u}^k_* - \sum_{\text{r.e}} \lambda^e_k\, \mathbf{grad}_k\, S^e_k \quad \text{for } |k| \geq 1\,; \tag{5.5}$$

$$\text{with:}\quad \boldsymbol{u}^k_* = \boldsymbol{u}^k_{BS} - \mathbf{grad}_k\, \varphi^k_* \in \boldsymbol{X}^{\text{reg}}_{(k)}(\omega) \quad \forall k.$$

The above decompositions are hardly adapted to numerical computations, as the singular fields used in them depend on the mode and contain cutoff functions. This point will be addressed below. However, they have nice properties which we now state.

Lemma 5.1. *The singularity coefficients λ^j_k satisfy the bounds:*

$$|\lambda^e_0| \lesssim \|\boldsymbol{u}^0\|_{\boldsymbol{X},(0)},\ \forall \boldsymbol{e}, \quad |\lambda^c_0| \lesssim \|\boldsymbol{u}^0\|_{\boldsymbol{X},(0)},\ \forall \boldsymbol{c}; \tag{5.6}$$

$$|\lambda^e_k| \lesssim |k|^{\alpha_e - 1}\, \|\boldsymbol{u}^k\|_{\boldsymbol{X},(k)},\ \forall \boldsymbol{e},\ \forall |k| \geq 1. \tag{5.7}$$

As a consequence, $\|\lambda^e_k\, \mathbf{grad}_k\, S^e_k\|_{\boldsymbol{X},(k)} \lesssim \|\boldsymbol{u}^k\|_{\boldsymbol{X},(k)}$ and $\|\boldsymbol{u}^k_*\|_{\boldsymbol{X},(k)} \lesssim \|\boldsymbol{u}^k\|_{\boldsymbol{X},(k)}$; thus, the series $\sum \boldsymbol{u}^k_*\, \mathrm{e}^{\mathrm{i}k\theta}$ and $\sum \lambda^e_k\, (\mathbf{grad}_k\, S^e_k)\, \mathrm{e}^{\mathrm{i}k\theta}$ for any reentrant edge $\boldsymbol{e}$ converge in $\boldsymbol{X}(\Omega)$.

Proof. Let $f^k := \operatorname{div}_k(\boldsymbol{u}^k - \boldsymbol{u}^k_{BS}) = -\Delta_k \varphi^k$. By the continuity estimate (2.29), we have $\|f^k\|_{0,1} \lesssim \|\boldsymbol{u}^k\|_{\boldsymbol{X},(k)}$. The coefficients λ^j_k are clearly the same in (5.4) or (5.5) and in (5.1); yet the latter satisfy: $|\lambda^j_k| \lesssim \|f^k\|_{0,1}$ for $|k| \leq 1$ and $|\lambda^e_k| \lesssim |k|^{\alpha_e - 1}\, \|f^k\|_{0,1}$ for $|k| \geq 2$, as shown in [20], respectively Equations (36,49) and Lemma 3.1 of this Reference. Hence (5.6) and (5.7).

On the other hand, it is easy to check (calculating like in Lemma 5.5 of [3]) that $\|\, \mathbf{grad}_k\, S^e_k\|_{\boldsymbol{X},(k)} = \|\Delta_k\, S^e_k\|_{0,1} \lesssim |k|^{1-\alpha_e}$. Thus, $\|\lambda^e_k\, \mathbf{grad}_k\, S^e_k\|_{\boldsymbol{X},(k)} \lesssim \|\boldsymbol{u}^k\|_{\boldsymbol{X},(k)}$ for all $\boldsymbol{e}$ and finally $\|\boldsymbol{u}^k_*\|_{\boldsymbol{X},(k)} \lesssim \|\boldsymbol{u}^k\|_{\boldsymbol{X},(k)}$. □

Similar decompositions and estimates hold in the magnetic case (recall the absence of vertex singularities in this case), with $S^e_k(\rho_e, \phi_e) = \eta_e(\rho_e)\, \mathrm{e}^{-|k|\,\rho_e}\, \rho_e^{\alpha_e}\, \cos(\alpha_e \phi_e)$.

5.2. **Regularity results.** As we remarked in Theorem 2.10, the global regularity of the electromagnetic field is quite low. In order to have good approximation properties, one has to estimate the regularity of the *regular* part of the field, which is approximated by finite elements. We shall see that it can be limited by *all* edges and vertices — not only the reentrant or sharp ones. Moreover, even with very smooth data, it can be hardly better than $\boldsymbol{H}^1$; this condition requires the use of the modified Clément operator defined in §6.2.

Definition 5.2. The space $\boldsymbol{X}^s_{(k)}(\omega)$, for $s \geq 1$, is the subspace of all $\boldsymbol{u}^k \in \boldsymbol{X}_{(k)}(\omega)$ whose regular part $\boldsymbol{u}^k_*$, as defined in (5.4) or (5.5), belongs to $\boldsymbol{H}^s_{(k)}(\omega)$. Its norm is chosen as:

$$k = 0: \qquad \|\boldsymbol{u}^0\|^2_{\boldsymbol{X},s,(0)} := \|\boldsymbol{u}^0_*\|^2_{s,(0)} + \sum_{\text{r.e.}} |\lambda^e_0|^2 + \sum_{\text{s.v.}} |\lambda^c_0|^2\,; \tag{5.8}$$

$$|k| \geq 1: \qquad \|\boldsymbol{u}^k\|^2_{\boldsymbol{X},s,(k)} := \|\boldsymbol{u}^k_*\|^2_{s,(k)} + \sum_{\text{r.e.}} |k|^{2(1-\alpha_e)}\, |\lambda^e_k|^2\,. \tag{5.9}$$

As a particular case, $\boldsymbol{X}^1_{(k)}(\omega) = \boldsymbol{X}_{(k)}(\omega)$, and the norms are equivalent.

The space $\boldsymbol{X}^s(\Omega)$ is the subspace of all $\boldsymbol{u} \in \boldsymbol{X}(\Omega)$ such that its Fourier coefficients $\boldsymbol{u}^k$ belong to $\boldsymbol{X}^s_{(k)}(\omega)$ for all k. It is endowed with the canonical norm $\|\boldsymbol{u}\|^2_{\boldsymbol{X},s} := \sum_{k\in\mathbb{Z}} \|\boldsymbol{u}^k\|^2_{\boldsymbol{X},s,(k)}$.

The finiteness of the norm $\|\boldsymbol{u}\|_{\boldsymbol{X},s}$ if $\boldsymbol{u}^k \in \boldsymbol{X}^s_{(k)}(\omega)$ for all k follows from Lemma 5.1. The latter, together with the well-known [2, §4] equivalence of the norms $\|\cdot\|_{\boldsymbol{X}}$ and $\|\cdot\|_1$ on $\boldsymbol{X}^{\text{reg}}(\Omega)$, hence of $\|\cdot\|_{\boldsymbol{X},(k)}$ and $\|\cdot\|_{1,(k)}$ on $\boldsymbol{X}^{\text{reg}}_{(k)}(\omega)$, yields the equivalence of norms $\|\cdot\|_{\boldsymbol{X}}$ and $\|\cdot\|_{\boldsymbol{X},1}$ on $\boldsymbol{X}(\Omega)$.

Definition 5.3. Let $\nu^{k;\ell}_c$ be the ℓ-th singularity exponent of the Laplacian (with Dirichlet boundary condition) at the conical vertex $\boldsymbol{c}$ for the Fourier mode k, i.e. the ℓ-th smallest positive root of $P^k_\nu(\cos\pi/\beta_c) = 0$. (Thus, $\nu_c = \nu^{0;1}_c$.)

The *limiting regularisation exponent* of the Laplacian at the mode k is $s^k_\Delta := \min \mathbb{S}_k$, where the set $\mathbb{S}_k$ is defined as a function of $|k|$ as:

$$\begin{aligned}
\mathbb{S}_0 \quad &= \quad \Big\{\alpha_e : \boldsymbol{e} \text{ salient edge}\ ;\ 2\,\alpha_e : \boldsymbol{e} \text{ reentrant edge}\ ; \\
&\qquad \nu^{0;1}_c + \tfrac{1}{2} : \boldsymbol{c} \text{ non-sharp vertex}\ ;\ \nu^{0;2}_c + \tfrac{1}{2} : \boldsymbol{c} \text{ sharp vertex}\Big\}\ ; \\
\mathbb{S}_1 \quad &= \quad \Big\{\alpha_e : \boldsymbol{e} \text{ salient edge}\ ;\ 2\,\alpha_e : \boldsymbol{e} \text{ reentrant edge}\ ;\ \nu^{1;1}_c + \tfrac{1}{2} : \boldsymbol{c} \text{ any vertex}\Big\}\ ; \\
\mathbb{S}_k \quad &= \quad \Big\{\alpha_e : \boldsymbol{e} \text{ salient edge}\ ;\ 2\,\alpha_e : \boldsymbol{e} \text{ reentrant edge}\Big\}, \quad k \geq 2.
\end{aligned}$$

The limiting regularisation exponent of the Maxwell operator at the mode 0 is

$$\begin{aligned}
s^0_\star \quad := \quad \min\Big(&\alpha_e : \boldsymbol{e} \text{ salient edge}\ ;\ 2\,\alpha_e : \boldsymbol{e} \text{ reentrant edge}\ ; \\
&\nu^{0;1}_c + \tfrac{1}{2} : \boldsymbol{c} \text{ non-sharp vertex}\ ;\ \nu^{0;1}_c + \tfrac{3}{2} : \boldsymbol{c} \text{ sharp vertex}\Big)\ ;
\end{aligned}$$

while for the modes $|k| \geq 1$, one has $s^k_\star = s^k_\Delta$. Notice [12, p. 48] that the only exponents ν whose value is possibly less than 2 are $\nu^{0;1}_c$, $\nu^{0;2}_c$, and $\nu^{1;1}_c$, the latter two being always greater than 1. This is the reason why, for $|k| \geq 2$, regularity is limited by the edges only.

The global limiting regularisation exponent of the Maxwell operator is $s_\star := \min(s^0_\star, s^1_\star) = \min_{k\in\mathbb{Z}} s^k_\star$.

Remark 5.4. We see that $s_\star < 2$ as soon as one edge aperture is greater than $\pi/2$. As for the conical vertices, there holds $s^k_\star < 2$ for $|k| = 0,\ 1$ when the aperture is greater than $\vartheta_{|k|}$, with $\vartheta_0 \simeq 68°8'$ and $\vartheta_1 \simeq 114°48'$. As a consequence, $\mathbb{P}_1$ finite elements will be sufficient for non-mixed formulations (including correction methods) in most situations. When using mixed formulations, however, one has to use $\mathbb{P}_2$ elements for the field (and $\mathbb{P}_1$ for the multiplier) in order to have the theoretical framework for proving convergence, see Lemma 4.2 and Propositions 4.3 & 4.4. This is what we assume in the rest of this article.

Proposition 5.5. *Let $\boldsymbol{f} \in \boldsymbol{X}(\Omega)'$ and $g \in L^2(\Omega)$, and let $(\boldsymbol{u}, p) \in \boldsymbol{X}(\Omega) \times L^2(\Omega)$ be the solution to:*

$$a(\boldsymbol{u}, \boldsymbol{v}) + b(\boldsymbol{v}, p) = \langle \boldsymbol{f}, \boldsymbol{v} \rangle, \quad \forall \boldsymbol{v} \in \boldsymbol{X}(\Omega), \tag{5.10}$$

$$b(\boldsymbol{u}, q) = (g \mid q), \quad \forall q \in L^2(\Omega). \tag{5.11}$$

If $\boldsymbol{f} \in \boldsymbol{H}^{s-2}(\Omega)$ and $g \in H^{s-1}(\Omega)$ for some $s \in [1, s_\star^k)$, then $\boldsymbol{u}^k \in \boldsymbol{X}^s_{(k)}(\omega)$ and $p^k \in H^s_{(k)}(\omega)$. Consequently, $\boldsymbol{u} \in \boldsymbol{X}^s(\Omega)$ and $p \in H^s(\Omega)$ for $s < s_\star$.

Proof. Thanks to [2], we can adapt the result of [25, Thm 5.2] to the case of the axisymmetric domain: the (non-unique) Birman–Solomyak decomposition (2.22) can be chosen such that

$$\begin{aligned} &\boldsymbol{f} \in \boldsymbol{H}^{s-2}(\Omega) \text{ and } g \in H^{s-1}(\Omega) \implies \\ &\quad \Delta\varphi \in H^{s-1}(\Omega) \text{ and } \boldsymbol{u}_{BS} \in \boldsymbol{H}^{\sigma+1}(\Omega), \text{ and } p \in H^{\tau+1}(\Omega), \\ &\qquad \text{for: } \sigma \le s-1 \text{ and } \sigma < \min\left\{\alpha_e, \mu_c^D + \tfrac{1}{2}, \mu_c^N + \tfrac{1}{2}\right\}, \\ &\qquad\quad \tau \le s-1 \text{ and } \tau < \min\left\{\alpha_e, \mu_c^D + \tfrac{1}{2}\right\}, \end{aligned}$$

where μ_c^D (resp. μ_c^N) is the smallest singularity exponent of the Laplacian with Dirichlet (resp. Neumann) boundary condition at the vertex $\boldsymbol{c}$. Moreover, this decomposition is continuous with respect to the norms $\|\boldsymbol{f}\|_{s-2}$ and $\|g\|_{s-1}$. We remark that μ_c^D coincides with $\nu_c^{0;1}$; moreover, it is known [30] that $\mu_c^N \ge \underline{\mu}^N > 0.84$. Thus, at least for $s < 2.34$, there holds $\boldsymbol{u}_{BS} \in \boldsymbol{H}^s(\Omega)$ and $p \in H^s(\Omega)$ iff $s < 1 + \alpha_e$ (reentrant edges) and $s < \nu_c^{0;1} + \frac{3}{2}$ (sharp vertices).

Reasoning mode by mode (see Remark 2.11), we thus have $\boldsymbol{u}^k_{BS} \in \boldsymbol{H}^s_{(k)}(\omega)$, $p^k \in H^s_{(k)}(\omega)$ and $\Delta_k\, \varphi^k \in H^{s-1}_{(k)}(\omega)$. By Thms II.4.10 and II.4.11 of [12], the latter property implies that φ^k_* (defined in (5.1)) belongs to $H^{s+1}_{(k)}(\omega)$, i.e. $\mathbf{grad}_k\, \varphi^k_* \in \boldsymbol{H}^s_{(k)}(\omega)$ for $s < s^k_\Delta$. Finally, we notice that for any reentrant edge, $2\alpha_e < 1 + \alpha_e$; and one can check that $\nu_c^{0;1} + 1 \le \nu_c^{0;2}$ for all values of the aperture π/β_c, the equality being possible only if $\beta_c = 1$. (For the values $\nu \le 2$, see Figure II.4.1 in [12]). Hence the conclusion. □

Proposition 5.6. *Let $\boldsymbol{u} \in \boldsymbol{X}(\Omega)$ and $s < s_\star$; then $\boldsymbol{u}$ belongs to $\boldsymbol{X}^s(\Omega)$ iff $(\mathbf{curl}\, \boldsymbol{u}, \operatorname{div} \boldsymbol{u}) \in \boldsymbol{H}^{s-1}(\Omega) \times H^{s-1}(\Omega)$.*

Proof. Assume $(\mathbf{curl}\, \boldsymbol{u}, \operatorname{div} \boldsymbol{u}) \in \boldsymbol{H}^{s-1}(\Omega) \times H^{s-1}(\Omega)$. It is easy to check that $(\boldsymbol{u}, 0)$ is the solution to (5.10,5.11), with $g = \operatorname{div} \boldsymbol{u}$ and $\boldsymbol{f} = \mathbf{curl}\,\mathbf{curl}\, \boldsymbol{u} - \mathbf{grad} \operatorname{div} \boldsymbol{u} \in \boldsymbol{H}^{s-2}(\Omega)$. Hence $\boldsymbol{u} \in \boldsymbol{X}^s(\Omega)$ by the previous proposition.

Conversely, $\boldsymbol{u} \in \boldsymbol{X}(\Omega)$ implies $(\mathbf{curl}_k\, \boldsymbol{u}^k_*, \operatorname{div}_k \boldsymbol{u}^k_*) \in \boldsymbol{H}^{s-1}_{(k)}(\omega) \times H^{s-1}_{(k)}(\omega)$ for all k. As far as the singular parts are concerned, there holds $\mathbf{curl}_k\, \mathbf{grad}_k\, S^j_k = 0$ and $\operatorname{div}_k \mathbf{grad}_k\, S^j_k = \Delta_k\, S^j_k$. When $\boldsymbol{j}$ is the reentrant edge $\boldsymbol{e}$, this function vanishes near the axis and is smooth everywhere except near $\boldsymbol{e}$. In addition, in ω_e, one finds by direct computations:

$$\Delta_k\, S^e_k = \Delta_\perp S^e_k + \text{l.s.t.} = \mathrm{e}^{-|k|\,\rho_e}\, \rho_e^{\alpha_e - 1}\, \sin(\alpha_e \phi_e)\, \{|k|\,\rho_e - (1 + 2\alpha_e)\,|k|\} + \text{l.s.t.}$$

Here, $\Delta_\perp$ denotes the Laplacian in the (r, z) plane, and l.s.t. means less singular terms. Therefore, $\Delta_k\, S^e_k \in \underline{H}^{\alpha_e}(\omega_e)$, and globally $\Delta_k\, S^e_k \in H^{s-1}_{(k)}(\omega)$ since $\alpha_e >$

$2\alpha_e - 1 \geq s - 1$. Now, for a sharp vertex $\boldsymbol{c}$, one checks that $\Delta_0 S_0^c$ vanishes in ω_c, and is smooth elsewhere. All together, we have thus $(\mathbf{curl}_k\, \boldsymbol{u}^k, \mathrm{div}_k\, \boldsymbol{u}^k) \in \boldsymbol{H}^{s-1}_{(k)}(\omega) \times H^{s-1}_{(k)}(\omega)$ for all k, i.e. $(\mathbf{curl}\, \boldsymbol{u}, \mathrm{div}\, \boldsymbol{u}) \in \boldsymbol{H}^{s-1}(\Omega) \times H^{s-1}(\Omega)$. $\square$

The above results can be rephrased for the magnetic boundary condition, provided one adapts the results of [25] to this case, and uses the description of conical singularities from [30].

6. Practical approximation results

6.1. **Mode-independent singular fields.** For the practical purpose of the SCM, the singular parts can be described with other singular fields $\mathbf{x}_S^{k,j}$. Generally speaking, these fields should be easy to compute and satisfy the following conditions.

(1) They are independent of k for $|k| \geq 2$.
(2) They are smooth (i.e., at least $\mathcal{C}^{\kappa+1}$ if $\mathbb{P}_\kappa$ elements are used) away from the relevant edge or vertex $\boldsymbol{j}$.
(3) Near the edge or vertex $\boldsymbol{j}$, they are equal to $-\,\mathbf{grad}_k\, S_k^j + \boldsymbol{w}_j^k$, where $\boldsymbol{w}_j^k \in \boldsymbol{H}^{s_j}_{(k)}(\omega_j)$ for some $s_j > 1$ large enough.
(4) They satisfy the suitable condition of the mode k on γ_a.
(5) They satisfy the electric boundary condition on γ_b.

The last two conditions imply that the regular and singular parts of the field satisfy separately the relevant boundary conditions on $\partial\omega$, so the latter can be treated as essential for the regular part. Conditions 2 and 3 ensure, first, that the singularity coefficients will be the same as in (5.4) and (5.5), and then, that the regular part will not be "polluted" by terms not smooth enough to guarantee a good convergence rate of the finite elements. Finally, the first condition appears mandatory in order to keep the overall cost of the method at a reasonable level. There is, however, a price to pay: one has to assume some extra regularity in θ for the field.

We now construct such singular fields. Let $\mathbf{S}_e = -(r/a_e)\, \mathbf{grad}_0\, [\rho_e^{\alpha_e}\, \sin(\alpha_e \phi_e)]$ and $\mathbf{S}_c = -\,\mathbf{grad}_0\, [\rho_c^{\nu_c}\, P_{\nu_c}(\cos\phi_c)]$; their expression in the basis $(\mathbf{e}_r, \mathbf{e}_\theta, \mathbf{e}_z)$ writes:

$$\mathbf{S}_e = -\frac{r}{a_e}\, \alpha_e\, \rho_e^{\alpha_e - 1} \begin{pmatrix} \sin((\alpha_e - 1)\phi_e - \phi_e^0) \\ 0 \\ \cos((\alpha_e - 1)\phi_e - \phi_e^0) \end{pmatrix}; \tag{6.1}$$

$$\mathbf{S}_c = -\rho^{\nu_c - 1} \begin{pmatrix} \nu_c\, P_{\nu_c}(\cos\phi_c)\sin\phi_c + P^1_{\nu_c}(\cos\phi_c)\cos\phi_c \\ 0 \\ -\nu_c\, P_{\nu_c}(\cos\phi_c)\cos\phi_c + P^1_{\nu_c}(\cos\phi_c)\sin\phi_c \end{pmatrix}. \tag{6.2}$$

These fields obviously satisfy Conditions 1 and 2. For the vertex singular field $\mathbf{S}_c$, Condition 4 for $k = 0$ follows from the properties of Legendre functions, and Condition 3 is trivially satisfied since this field is exactly equal to $-\,\mathbf{grad}_0\, S_0^c$ in ω_c (where $\eta_c \equiv 1$). As far as $\mathbf{S}_e$ is concerned, its three components vanish on the axis thanks to the factor (r/a_e), hence Condition 4 is satisfied for all modes. Then, we shall see below that $\mathbf{S}_e + \mathbf{grad}_k\, S_k^e$ is equal in ω_e to $\rho_e^{\alpha_e}\, \boldsymbol{g}(\phi_e) +$ higher-order terms, cf. (6.9) below. This belongs to $\underline{\boldsymbol{H}}^{1+\alpha_e}(\omega_e) = \underline{\boldsymbol{H}}^{1+\alpha_e}_{(k)}(\omega_e)$, since the function $\boldsymbol{g}(\phi_e)$ and the higher-order terms are smooth.

On the other hand, $\mathbf{S}_e$ and $\mathbf{S}_c$ do not satisfy Condition 5, except on the side(s) of γ_b that touch the corner $\boldsymbol{e}$ or $\boldsymbol{c}$. Therefore, we take the following

Definition 6.1. Let $\mathbf{x}_S^{0,e} := -(r/a_e)\,\boldsymbol{\sigma}^e$, where $\boldsymbol{\sigma}^e$ is $\mathbf{grad}_0\,[\rho_e^{\alpha_e}\,\sin(\alpha_e\phi_e)]$ minus a lifting of its tangential trace on γ_b, which is smooth. Similarly, $\mathbf{x}_S^{0,c}$ is defined as $\mathbf{S}_c$ minus a lifting of its tangential trace on γ_b, which is smooth.

For the coherence of our notations, we set $\mathbf{x}_S^{k,e} = \mathbf{x}_S^{0,e}$ for all k; but let us emphasize that these fields are independent of k.

Lemma 6.2. *For any field $\boldsymbol{u} \in \boldsymbol{X}(\Omega)$, its Fourier coefficient $\boldsymbol{u}^k$ can be decomposed as:*

$$k = 0: \qquad \boldsymbol{u}^0 = \boldsymbol{u}_R^0 + \sum_{\text{r.e.}} \lambda_0^e\,\mathbf{x}_S^{0,e} + \sum_{\text{s.v.}} \lambda_0^c\,\mathbf{x}_S^{0,c}, \tag{6.3}$$

$$|k| \geq 1: \qquad \boldsymbol{u}^k = \boldsymbol{u}_R^k + \sum_{\text{r.e.}} \lambda_k^e\,\mathbf{x}_S^{k,e}, \tag{6.4}$$

$$\text{where:} \qquad \boldsymbol{u}_R^k \in \boldsymbol{X}_{(k)}^{\text{reg}}(\omega)\,; \quad \mathbf{x}_S^{k,e} \in \boldsymbol{X}_{(k)}(\omega),\ \forall k\,; \quad \mathbf{x}_S^{0,c} \in \boldsymbol{X}_{(0)}(\omega)\,;$$
$$\mathbf{x}_S^{k,e} + \mathbf{grad}_k\,S_k^e \in \underline{\boldsymbol{H}}_{(k)}^{1+\alpha_e}(\omega_e),\ \mathbf{x}_S^{k,e} \text{ is smooth elsewhere;}$$
$$\mathbf{x}_S^{0,c} = -\,\mathbf{grad}_0\,S_0^c \text{ in } \omega_c,\ \mathbf{x}_S^{0,c} \text{ is smooth elsewhere.}$$

In order to use the decompositions (6.3) and (6.4) for numerical computations, we have to check their stability in the various norms used for the fields. This is the purpose of the next two Lemmas.

Lemma 6.3. *The following bounds hold for all modes k and for $1 \leq s < 1 + \alpha_e$:*

$$\|\mathbf{x}_S^{k,e}\|_{\boldsymbol{X},(k)} \approx \|\mathbf{S}_e\|_{\boldsymbol{X},(k)} \lesssim 1 + |k|\,; \tag{6.5}$$

$$\|\mathbf{x}_S^{k,e} + \mathbf{grad}_k\,S_k^e\|_{0,-1} \approx \|\mathbf{S}_e + \mathbf{grad}_k\,S_k^e\|_{0,-1} \lesssim 1\,; \tag{6.6}$$

$$\|\mathbf{x}_S^{k,e} + \mathbf{grad}_k\,S_k^e\|_{s,1} \approx \|\mathbf{S}_e + \mathbf{grad}_k\,S_k^e\|_{s,1} \lesssim 1 + |k|^{s-\alpha_e}\,. \tag{6.7}$$

Proof. The estimate for $\mathbf{S}_e$ in (6.5) follows from simple calculations, see (7.3) and (7.4) below. As for $\mathbf{x}_S^{k,e}$, we remark that, as the tangential trace of $\mathbf{grad}_0\,[\rho_e^{\alpha_e}\,\sin(\alpha_e\phi_e)]$ on γ_b is smooth, there exists a continuous lifting in $H_1^{\kappa+1}(\omega)^3$. Then, multiplying by $-(r/a_e)$ we obtain a continuous lifting in $H_1^{\kappa+1}(\omega)^3 \cap V_1^1(\omega)^3$, whose norm is independent of k. Thus:

$$\|\mathbf{x}_S^{k,e} - \mathbf{S}_e\|_{s,1} + \|\mathbf{x}_S^{k,e} - \mathbf{S}_e\|_{0,-1} \lesssim 1, \quad \text{for } 1 \leq s < 2. \tag{6.8}$$

Note that neither $\mathbf{x}_S^{k,e}$ nor $\mathbf{S}_e$ belong to $H_1^s(\omega)^3$, but their difference does. Then, using the equivalence of the norms $\|\cdot\|_{\boldsymbol{X},(k)}$ and $\|\cdot\|_{1,(k)}$ for regular fields, we get the estimate for $\mathbf{x}_S^{k,e}$ in (6.5).

We now establish the estimates for $\mathbf{S}_e$ in (6.6) and (6.7); once we have them, the bounds for $\mathbf{x}_S^{k,e}$ will follow thanks to (6.8). The calculations are quite tedious, so we will only sketch them. The integrals defining the squared norms $\|\mathbf{S}_e+\mathbf{grad}_k\,S_k^e\|_{s,1}^2$ and $\|\mathbf{S}_e+\mathbf{grad}_k\,S_k^e\|_{0,-1}^2$ are made of three contributions, corresponding to different parts of the domain ω.

(1) The region where the cutoff function $\eta_e \equiv 0$. There, $\mathbf{grad}_k\,S_k^e = 0$, so the result is independent of k.
(2) The region where η_e varies. In this part of the domain, $\rho_e \geq \underline{\rho} > 0$ and $r \geq \underline{r} > 0$, so the norm of $\mathbf{grad}_k\,S_k^e$ (which is smooth there) in any Sobolev space is exponentially decreasing in $|k|$, and one can bound the contribution by a constant.

(3) The region where $\eta_e \equiv 1$, viz. ω_e. There, we have the following expression for $\mathbf{grad}_k\, S_k^e$ — for the sake of legibility, we generally drop the edge subscript e:

$$\mathrm{e}^{-|k|\,\rho}\,\rho^{\alpha-1}\begin{pmatrix}\alpha\,\sin((\alpha-1)\phi-\phi^0)-|k|\,\rho\,\sin(\alpha\phi)\,\cos(\phi+\phi^0)\\ \mathrm{i}k\,r^{-1}\,\rho\,\sin(\alpha\phi)\\ \alpha\,\cos((\alpha-1)\phi-\phi^0)-|k|\,\rho\,\sin(\alpha\phi)\,\sin(\phi+\phi^0)\end{pmatrix}.$$

To compare the previous expression with (6.1), we keep in mind that $r = a + \rho\cos(\phi+\phi^0)$, and that the function $\mathfrak{E}$ defined as $\mathfrak{E}(x) = (\mathrm{e}^x - 1)/x$ is smooth. Thus, we arrive at the following form for $\boldsymbol{w}_k^e := \mathbf{S}_e + \mathbf{grad}_k\, S_k^e$:

$$\begin{aligned}\boldsymbol{w}_k^e &= |k|\,\mathrm{e}^{-|k|\,\rho}\,\rho^{\alpha}\,\boldsymbol{g}_1(\phi)+|k|\,\mathfrak{E}(-|k|\,\rho)\,\rho^{\alpha}\,\boldsymbol{g}_2(\phi)\\ &\quad+\mathrm{i}k\,r^{-1}\,\mathrm{e}^{-|k|\,\rho}\,\rho^{\alpha}\,\boldsymbol{g}_3(\phi)+\rho^{\alpha}\,\boldsymbol{g}_4(\phi),\\ &:= \boldsymbol{w}_1+\boldsymbol{w}_2+\boldsymbol{w}_3+\boldsymbol{w}_4,\end{aligned}\tag{6.9}$$

where all the functions $\boldsymbol{g}_i(\phi)$ are smooth and independent of k.

We begin by estimating the norm $\|\boldsymbol{w}_k^e\|_{L^2_{-1}(\omega_e)}$. As we are away from the axis, it is bounded above and below by $\|\boldsymbol{w}_k^e\|_{L^2(\omega_e)}$. Actually, we calculate a L^p norm which will be needed below. The p-th power of the norm of $\boldsymbol{w}_1$ is bounded as

$$\begin{aligned}\|\boldsymbol{w}_1\|^p_{L^p(\omega_e)} &= \iint_{\omega_e}|k|^p\,\mathrm{e}^{-p\,|k|\,\rho}\,\rho^{p\alpha}\,|\boldsymbol{g}_1(\phi)|^p\,\rho\,\mathrm{d}\rho\,\mathrm{d}\phi\\ &\le C_{p,\alpha}\int_0^{+\infty}|k|^p\,\mathrm{e}^{-p\,|k|\,\rho}\,\rho^{p\alpha+1}\,\mathrm{d}\rho\\ &= C_{p,\alpha}\,|k|^p\int_0^{+\infty}\mathrm{e}^{-p\,\xi}\left(\frac{\xi}{|k|}\right)^{p\alpha+1}\frac{\mathrm{d}\xi}{|k|}\ \lesssim\ |k|^{p-p\alpha-2}.\end{aligned}$$

The calculation goes the same for $\boldsymbol{w}_2$ and $\boldsymbol{w}_3$ (as r^{-1} is bounded from above and from below in ω_e); as for $\boldsymbol{w}_4$, its norm is independent of k. Hence the bounds:

$$\forall p \le 2/(1-\alpha),\quad \|\boldsymbol{w}_k^e\|_{L^p(\omega_e)} \lesssim 1\,;\quad \|\boldsymbol{w}_k^e\|_{L^2_{-1}(\omega_e)} \approx \|\boldsymbol{w}_k^e\|_{L^2(\omega_e)} \lesssim 1.$$

The bound (6.6) follows, given that the contributions of the other parts of the domain are also bounded.

Then we proceed with the norm $\|\boldsymbol{w}_k^e\|_{H^s_1(\omega_e)}$. It is bounded above and below by $\|\boldsymbol{w}_k^e\|_{H^s(\omega_e)}$; in turn, a Sobolev injection allows us to bound the latter by $\|\boldsymbol{w}_k^e\|_{W^{2,p}(\omega_e)} \approx \|\boldsymbol{w}_k^e\|_{L^p(\omega_e)} + |\boldsymbol{w}_k^e|_{W^{2,p}(\omega_e)}$, with $p = 2/(3-s)$. If $s < 1+\alpha$, then $p < 2/(2-\alpha) < 2/(1-\alpha)$, and the $L^p(\omega_e)$ norm is bounded by a constant. To bound the $W^{2,p}(\omega_e)$ semi-norm, we have to estimate the $L^p(\omega_e)$ norms of

$$\frac{\partial^2 w}{\partial\rho^2},\quad \frac{1}{\rho}\,\frac{\partial^2 w}{\partial\rho\,\partial\phi}-\frac{1}{\rho^2}\,\frac{\partial w}{\partial\phi},\quad \frac{1}{\rho^2}\,\frac{\partial^2 w}{\partial\phi^2}+\frac{1}{\rho}\,\frac{\partial w}{\partial\rho},$$

where w is any cylindrical component of any $\boldsymbol{w}_i$. It is easy to see that, for the components of $\boldsymbol{w}_1$, these functions are linear combinations of terms of the form

$$|k|^3\,\mathrm{e}^{-|k|\,\rho}\,\rho^{\alpha}\,h_1(\phi),\quad |k|^2\,\mathrm{e}^{-|k|\,\rho}\,\rho^{\alpha-1}\,h_2(\phi),\quad |k|\,\mathrm{e}^{-|k|\,\rho}\,\rho^{\alpha-2}\,h_3(\phi),$$

where the $h_i(\phi)$ are smooth and independent of k. Computing as above, we find that all these terms have their norm bounded by $|k|^{3-\alpha-2/p} = |k|^{s-\alpha}$. A similar calculation can be done for $\boldsymbol{w}_2$ and $\boldsymbol{w}_3$ (as r^{-1} is smooth in ω_e, there holds

$\|\boldsymbol{w}_3\|_{W^{2,p}(\omega_e)} \lesssim \|k\,\mathrm{e}^{-|k|\,\rho}\,\rho^\alpha\,\boldsymbol{g}_3(\phi)\|_{W^{2,p}(\omega_e)})$; while the norm of $\boldsymbol{w}_4$ is once more constant. Finally:

$$\|\boldsymbol{w}_k^e\|_{H_1^s(\omega_e)} \lesssim \|\boldsymbol{w}_k^e\|_{W^{2,p}(\omega_e)} \lesssim 1 + |k|^{s-\alpha}.$$

This bound, together with the estimates on the contributions of the other parts of the domain, leads to (6.7). □

Of course, a similar result holds for the sharp vertices at the mode 0.

Lemma 6.4. *Assume that $1 \le s < \nu_c^{0;1} + \frac{3}{2}$. The singular parts associated to the sharp vertices satisfy:*

(6.10)
$$\|\mathbf{x}_S^{0,c}\|_{\boldsymbol{X},(0)} \approx \|\mathbf{S}_c\|_{\boldsymbol{X},(0)} \lesssim 1\,; \quad \|\mathbf{x}_S^{0,c} + \mathbf{grad}_0\, S_0^c\|_{s,1} \approx \|\mathbf{S}_c + \mathbf{grad}_0\, S_0^c\|_{s,1} \lesssim 1.$$

As a consequence of the previous two Lemmas and the definition of the norm $\|\cdot\|_{\boldsymbol{X},s,(k)}$ we have:

Lemma 6.5. *Assume that $1 \le s < s_\star$. The regular and singular parts in* (6.3) *and* (6.4) *satisfy, for all $\boldsymbol{u} \in \boldsymbol{X}(\Omega)$ or $\boldsymbol{X}^s(\Omega)$:*

$$\|\boldsymbol{u}_R^0\|_{\boldsymbol{X},(0)} \lesssim \|\boldsymbol{u}^0\|_{\boldsymbol{X},(0)}, \quad \|\lambda_0^j\,\mathbf{x}_S^{0,j}\|_{\boldsymbol{X},(0)} \lesssim \|\boldsymbol{u}^0\|_{\boldsymbol{X},(0)}\,; \tag{6.11}$$

$$\|\boldsymbol{u}_R^0\|_{s,1} \lesssim \|\boldsymbol{u}^0\|_{\boldsymbol{X},s,(0)}\,; \tag{6.12}$$

for the mode $k = 0$, while for $|k| \ge 1$ there holds:

$$\|\boldsymbol{u}_R^k\|_{\boldsymbol{X},(k)} \lesssim (1 + |k|^{\alpha^\star})\,\|\boldsymbol{u}^k\|_{\boldsymbol{X},(k)}, \tag{6.13}$$

$$\|\lambda_k^e\,\mathbf{x}_S^{k,e}\|_{\boldsymbol{X},(k)} \lesssim (1 + |k|^{\alpha_e})\,\|\boldsymbol{u}^k\|_{\boldsymbol{X},(k)}\,; \tag{6.14}$$

$$\|\boldsymbol{u}_R^k\|_{s,1} \lesssim (1 + |k|^{s-1})\,\|\boldsymbol{u}^k\|_{\boldsymbol{X},s,(k)}\,, \quad \|\boldsymbol{u}_R^k\|_{0,-1} \lesssim \|\boldsymbol{u}^k\|_{\boldsymbol{X},s,(k)}\,. \tag{6.15}$$

Above, we have set $\alpha^\star := \max\{\alpha_e < 1\}$. As a consequence, the series $\sum \boldsymbol{u}_R^k\,\mathrm{e}^{\mathrm{i}k\theta}$ and $\sum \lambda_k^e\,\mathbf{x}_S^{k,e}\,\mathrm{e}^{\mathrm{i}k\theta}$ for any reentrant edge $\boldsymbol{e}$, converge in $\boldsymbol{X}(\Omega)$ for all $\boldsymbol{u} \in H^{1,\boldsymbol{X}}(\Omega)$.

For the numerical implementation, one can also orthonormalise the basis $(\mathbf{x}_S^{k,j})_j$ and compute basis vectors $(\mathbf{x}_{S\perp}^{k,j})_j$ which are orthogonal to one another and to the regular space $\boldsymbol{X}_{(k)}^{\mathrm{reg}}(\omega)$ with respect to the bilinear form $a_k(\cdot,\cdot)$ for $|k| \le 2$. This is the approach taken, at the discrete level, in §7. The adaptation to the magnetic boundary condition is once more immediate, with $\mathbf{S}_e = -(r/a_e)\ \mathbf{grad}_0\,[\rho_e^{\alpha_e}\ \cos(\alpha_e\phi_e)]$.

6.2. **The Clément operator.** We briefly explain its construction, which follows §§4.3 and 4.4 of [8]. For each node $\boldsymbol{a}_i$ in the principal lattice of the triangulation, one selects a triangle T_i which contains $\boldsymbol{a}_i$. Then, one introduces π_i, the L_1^2-orthogonal projection operator onto $\mathbb{P}_\kappa(T_i)$: for any $w \in L_1^1(T_i)$, $\pi_i w \in \mathbb{P}_\kappa(T_i)$ and

$$\forall p \in \mathbb{P}_\kappa(T_i), \quad \iint_{T_i} (w - \pi_i w)\,p\,r\,\mathrm{d}\omega = 0.$$

Let us begin with the case of regular fields. In order to enforce the various boundary conditions for the different modes, one classifies the nodes into four categories:

1. the interior nodes, which do not stand on $\partial\omega$;
2. the nodes standing on the axis γ_a, excluding the extremities;
3. those on the sides of the physical boundary γ_b, excluding the corners;
4. the corners, at the intersection of γ_a and γ_b, or of two sides of γ_b;

one denotes $\mathcal{K}_\ell = \{i :$ the node $\boldsymbol{a}_i$ is of category $\ell\}$, for $\ell = 1, \ldots, 4$. Notice that: (i) the outgoing normal and tangent vectors $\boldsymbol{\nu}_i$ and $\boldsymbol{\tau}_i$ are unambiguously defined at each node of category 2 or 3, since the sides are straight; (ii) the regular fields vanish at the nodes of category 4.

Definition 6.6. Let φ_i be the basis function associated with $\boldsymbol{a}_i$. The regularisation operator $\boldsymbol{\Pi}^\sigma_{h;k} : \boldsymbol{L}^2_1(\omega) \to \mathbb{X}^{\mathrm{reg};h}_{(k)}$ for the mode k and the boundary condition σ ($\sigma = \nu$ is the electric b.c., $\sigma = \tau$ is the magnetic b.c.) is the sum $\boldsymbol{\Pi}^\sigma_{h;k} := \boldsymbol{\Pi}^1_h + \boldsymbol{\Pi}^2_{h;k} + \boldsymbol{\Pi}^{3;\sigma}_h$, where:

$$\boldsymbol{\Pi}^1_h \boldsymbol{u}(\boldsymbol{x}) := \sum_{i\in\mathcal{K}_1} \{\pi_i u_r(\boldsymbol{a}_i)\,\mathrm{e}_r + \pi_i u_\theta(\boldsymbol{a}_i)\,\mathrm{e}_\theta + \pi_i u_z(\boldsymbol{a}_i)\,\mathrm{e}_z\}\ \varphi_i(\boldsymbol{x})\,; \tag{6.16}$$

$$\boldsymbol{\Pi}^2_{h;0} \boldsymbol{u}(\boldsymbol{x}) := \sum_{i\in\mathcal{K}_2} \pi_i u_z(\boldsymbol{a}_i)\,\mathrm{e}_z\,\varphi_i(\boldsymbol{x})\,; \tag{6.17}$$

$$\boldsymbol{\Pi}^2_{h;\pm1} \boldsymbol{u}(\boldsymbol{x}) := \sum_{i\in\mathcal{K}_2} \pi_i u_\pm(\boldsymbol{a}_i)\,\mathrm{e}_\pm\,\varphi_i(\boldsymbol{x})\,; \quad \boldsymbol{\Pi}^2_{h;k} \boldsymbol{u}(\boldsymbol{x}) := 0 \text{ for } |k| \geq 2\,; \tag{6.18}$$

$$\boldsymbol{\Pi}^{3;\nu}_h \boldsymbol{u}(\boldsymbol{x}) := \sum_{i\in\mathcal{K}_3} \pi_i u_\nu(\boldsymbol{a}_i)\,\boldsymbol{\nu}_i\,\varphi_i(\boldsymbol{x})\,; \tag{6.19}$$

$$\boldsymbol{\Pi}^{3;\tau}_h \boldsymbol{u}(\boldsymbol{x}) := \sum_{i\in\mathcal{K}_3} \{\pi_i u_\tau(\boldsymbol{a}_i)\,\boldsymbol{\tau}_i + \pi_i u_\theta(\boldsymbol{a}_i)\,\mathrm{e}_\theta\}\ \varphi_i(\boldsymbol{x}). \tag{6.20}$$

This operator automatically satisfies the electric or magnetic boundary condition on the physical boundary γ_b, as well as the boundary condition for regular fields of the mode k on the axis γ_a. Let us investigate its approximation properties.

Proposition 6.7. *Let $\boldsymbol{u} \in H^s_1(\omega)^3 \cap V^1_1(\omega)^3$ such that $\boldsymbol{u}\times\boldsymbol{n} = 0$, resp. $\boldsymbol{u}\cdot\boldsymbol{n}$ on γ_b. The following estimate holds for $s \in [1, \kappa + 1]$:*

$$h^{-1}\,\left\|\boldsymbol{u} - \boldsymbol{\Pi}^\sigma_{h;k}\boldsymbol{u}\right\|_{0,1} + \left|\!\left|\!\left|\boldsymbol{u} - \boldsymbol{\Pi}^\sigma_{h;k}\boldsymbol{u}\right|\!\right|\!\right|_{1,1} \lesssim h^{s-1}\,\{\|\boldsymbol{u}\|_{s,1} + \|\boldsymbol{u}\|_{0,-1}\}\,. \tag{6.21}$$

Hence, for $|k| \geq 2$, $s \in [1, 2]$ and $\boldsymbol{u} \in \boldsymbol{H}^s_{(k)}(\omega) \cap \boldsymbol{X}_{(k)}(\omega)$:

$$\left\|\boldsymbol{u} - \boldsymbol{\Pi}^\sigma_{h;k}\boldsymbol{u}\right\|^2_{1,(k)} \lesssim h^{2s-2}\,(1 + |k|^2)\,\left\{\|\boldsymbol{u}\|^2_{s,1} + \|\boldsymbol{u}\|^2_{0,-1}\right\}. \tag{6.22}$$

Proof. For integral values of s, the estimate (6.21) is obtained by following the proof of [8] step by step. To extend it to other values, we rely on interpolation arguments in suitable scales of weighted spaces. We give the detail in the case $s \in (1, 2)$, which is the one needed in the framework of this article.

It is known (see §2.4) that the following spaces are equal, algebraically and topologically, for $1 < s < 2$:

$$V^s_1(\omega) = H^s_{(1)}(\omega) = H^s_1(\omega) \cap V^1_1(\omega) = \{w \in H^s_1(\omega) : w = 0 \text{ on } \gamma_a\}. \tag{6.23}$$

For $s = 1$, the first two equalities hold; for $s = 2$, the last three spaces are equal, while $V^2_1(\omega)$ is algebraically and topologically embedded in them. Thus, for $s \in (1, 2)$, $H^s_1(\omega) \cap V^1_1(\omega)$ appears as the interpolate of order $s - 1$ between $V^1_1(\omega)$ and $H^2_1(\omega) \cap V^1_1(\omega)$: this amounts to do interpolation in the scale $(H^s(\Omega))_s$ in the special case of scalar functions having only one non-zero Fourier mode, corresponding to $k = 1$.

Assume now that $\boldsymbol{u} \in H^2_1(\omega)^3 \cap V^1_1(\omega)^3$, with $\boldsymbol{u} \times \boldsymbol{n}_{|\gamma_b} = 0$. The magnetic boundary condition can be handled in the same manner. The bound (6.21) holds for $s = 1$ and $s = 2$; the above interpolation property implies that it is also true for all $s \in [1,2]$. As the definition (2.21) implies: $\|\cdot\|^2_{1,(k)} \lesssim (1+|k|^2) \left|\!\left|\!\left| \cdot \right|\!\right|\!\right|_{1,1}$, the estimate (6.22) follows. In order to extend it to the case of $\boldsymbol{u} \in \boldsymbol{H}^s_{(k)}(\omega) \cap \boldsymbol{X}_{(k)}(\omega)$, i.e., $\boldsymbol{u} \in H^s_1(\omega)^3 \cap V^1_1(\omega)^3$ with $\boldsymbol{u} \times \boldsymbol{n}_{|\gamma_b} = 0$, we need a density argument which we now give.

First, we know [2, Proposition 4.7 & Remark 4.3] that $\boldsymbol{X}(\Omega) \cap \mathcal{C}^\infty(\Omega)^3$ is dense within $\boldsymbol{X}^{\mathrm{reg}}(\Omega)$; with suitable adaptations, the same proof shows the density in $\boldsymbol{X}(\Omega) \cap \boldsymbol{H}^2(\Omega)$. Then, an interpolation argument in the scale $\boldsymbol{H}^s(\Omega)$ yields the density in $\boldsymbol{X}(\Omega) \cap \boldsymbol{H}^s(\Omega)$. As a consequence, $\boldsymbol{X}(\Omega) \cap \boldsymbol{H}^2(\Omega)$ is dense in $\boldsymbol{X}(\Omega) \cap \boldsymbol{H}^s(\Omega)$. For the modes $|k| \geq 2$, this means that $\boldsymbol{X}_{(k)}(\omega) \cap \boldsymbol{H}^2_{(k)}(\omega) = \{\boldsymbol{u} \in V^2_1(\omega)^3 : \boldsymbol{u} \times \boldsymbol{n}_{|\gamma_b} = 0\}$ is dense within $\boldsymbol{X}_{(k)}(\omega) \cap \boldsymbol{H}^s_{(k)}(\omega)$. *A fortiori*, this is true for the bigger space $\{\boldsymbol{u} \in H^2_1(\omega)^3 \cap V^1_1(\omega)^3 : \boldsymbol{u} \times \boldsymbol{n}_{|\gamma_b} = 0\}$. □

The operators corresponding to the modes $|k| \leq 1$ can be estimated likewise (taking care of the conditions satisfied by the various components on the axis), giving an error in $h^{s-1}\|\boldsymbol{u}\|_{1,(k)}$. Thus, when the singular space is null, we get the approximation result (4.8) with:

$$\boldsymbol{X}^s_{(k)}(\omega) := \boldsymbol{H}^s_{(k)}(\omega) \cap \boldsymbol{X}_{(k)}(\omega), \quad \epsilon(s,h,k) = h^{s-1}(1+|k|). \tag{6.24}$$

Now we proceed with the general case. Near a geometrical singularity $\boldsymbol{j} = \boldsymbol{e}$ or $\boldsymbol{c}$, the numerical space $\mathbb{X}^h_{(k)}$ is spanned by the finite elements plus the *singular field* $\mathbf{S}_j$; away from it, the singular field is generally (according to the details of the numerical method) represented by an interpolate, or a lifting of its trace. This is of no importance, since $\mathbf{S}_j$ is $\mathcal{C}^\infty$ there, so the approximation will be as good as the finite elements allow. For instance, the Lagrange interpolation operator $\mathcal{I}_h$ satisfies the following bound for $\boldsymbol{w} \in H^s_1(\omega)^3 \cap V^1_1(\omega)^3$ and $s \in [2, \kappa+1]$:

$$h^{-1}\|\boldsymbol{w} - \mathcal{I}_h \boldsymbol{w}\|_{0,1} + \left|\!\left|\!\left| \boldsymbol{w} - \mathcal{I}_h \boldsymbol{w} \right|\!\right|\!\right|_{1,1} \lesssim h^{s-1}\|\boldsymbol{w}\|_{s,1},$$

see Proposition 6.1 in [39] and Proposition 4.1 in [8]. Globally, $\mathbb{X}^h_{(k)}$ can be thus described as:

$$\mathbb{X}^h_{(k)} = \mathbb{X}^{\mathrm{reg};h}_{(k)} \oplus \bigoplus_{\text{g.s.}} \operatorname{span} \mathbf{x}^{k,j;h}_S, \text{ where:}$$

$$\mathbf{x}^{k,j;h}_S \in \boldsymbol{X}_{(k)}(\omega), \quad \mathbf{x}^{k,j;h}_S = \mathbf{S}_j \text{ on } \omega_j, \quad \|\mathbf{x}^{k,j;h}_S - \mathbf{x}^{k,j}_S\|_{\boldsymbol{X},(k)} \lesssim h^\kappa (1+|k|).$$

Consequently, we can define a modified operator $\mathbf{\Pi}^\sigma_{h;k}$ on $\boldsymbol{X}_{(k)}(\omega)$ as follows:

$$\mathbf{\Pi}^\sigma_{h;k}: \quad \boldsymbol{u} = \boldsymbol{u}_R + \sum_{\text{g.s.}} \lambda_j \mathbf{x}^{k,j}_S \longmapsto \boldsymbol{\Pi}^\sigma_{h;k}\boldsymbol{u}_R + \sum_{\text{g.s.}} \lambda_j \mathbf{x}^{k,j;h}_S. \tag{6.25}$$

Combining Lemma 6.5 with the estimate (6.22) for regular fields, one immediately obtains:

Proposition 6.8. *The operator $\mathbf{\Pi}^\sigma_{h;k}$ satisfies the following bound, for any k and $\boldsymbol{u} \in \boldsymbol{X}^s_{(k)}(\omega)$:*

$$\left\|\boldsymbol{u} - \mathbf{\Pi}^\sigma_{h;k}\boldsymbol{u}\right\|^2_{\boldsymbol{X},(k)} \lesssim h^{2s-2}(1+|k|^{2s})\|\boldsymbol{u}\|^2_{\boldsymbol{X},s,(k)}. \tag{6.26}$$

Hence the general form of the approximation result (4.8):

$$\boldsymbol{X}^s_{(k)}(\omega) \text{ as in Definition 5.2,} \quad \epsilon(s,h,k) = h^{s-1}\,(1+|k|^s). \tag{6.27}$$

6.3. **Error estimates for the FUNFEM and FSCM.** We recall that the approximate numerical solution is reconstructed by the formula:

$$\{\boldsymbol{E}_h^{[N];n}, P_h^{[N];n}\}(r,\theta,z) := \frac{1}{\sqrt{2\pi}} \sum_{k=-N}^{N} \{\boldsymbol{E}_h^{k;n}, P_h^{k;n}\}(r,z)\,\mathrm{e}^{\mathrm{i}k\theta},$$

where $\left(\boldsymbol{E}_h^{k;n}\right)_n$, resp. $\left(\boldsymbol{E}_h^{k;n}, P_h^{k;n}\right)_n$ is the solution to the fully discrete mode-wise augmented (resp. mixed augmented) formulation.

Theorem 6.9. *Assume that $\boldsymbol{E} \in H^2(-\delta,T;\boldsymbol{X}^{s,q+\sigma}(\Omega)) \cap H^3(-\delta,T;\boldsymbol{H}^{0,\sigma}(\Omega))$ and $\boldsymbol{J} \in H^2(-\delta,T;\boldsymbol{H}^{0,\sigma}(\Omega))$, where $\sigma > \frac{1}{2}$, $s \in (1,s_\star)$ and q is defined according to the numerical method, in the following way:*

	UNFEM	SCM
Non-mixed	1	s
Mixed	2	$1+s$

Then we have the error estimates on the reconstructed solutions:

$$\|\partial_\tau \boldsymbol{E}_h^{[N];n} - \dot{\boldsymbol{E}}^n\|_0^2 + \|\boldsymbol{E}_h^{[N];n} - \boldsymbol{E}^n\|_{\boldsymbol{X}}^2 \le M_1\,(h^{2s-2} + \tau^2 + N^{-2\sigma}), \tag{6.28}$$

$$\|\boldsymbol{E}_h^{[N];n} - \boldsymbol{E}^n\|_0^2 \le M_2\,(h^{2s-2} + \tau^2 + N^{-2\sigma}). \tag{6.29}$$

The constants M_i depend on the norms of $\boldsymbol{E}$ and $\boldsymbol{J}$ in the aforementioned spaces.

Remark 6.10. Provided that the data $\boldsymbol{J}(t)$ and $\varrho(t)$ are smooth enough, we recall (see §5.2) that $\boldsymbol{E}(t)$ belongs automatically to $\boldsymbol{X}^s(\Omega)$, for $1 \le s < s_\star$.

Proof. Adding the estimates (4.9) or (4.19) from $k=-N$ to N, with the values of $\epsilon(s,h,k)$ given by (6.24) or (6.27), we obtain:

$$\|\partial_\tau \boldsymbol{E}_h^{[N];n} - \dot{\boldsymbol{E}}_\star^{[N];n}\|_0^2 + \|\boldsymbol{E}_h^{[N];n} - \boldsymbol{E}_\star^{[N];n}\|_{\boldsymbol{X}}^2 \lesssim M_N(\boldsymbol{E},\boldsymbol{J}) :=$$
$$h^{2s-2} \sum_{k=-N}^{N} (1+|k|^{2q})\,\|\boldsymbol{E}_\star^k\|^2_{H^2(\boldsymbol{X}^s_{(k)}(\omega))} + \tau^2\,\left[\|\boldsymbol{E}_\star^{[N]}\|^2_{H^3(\boldsymbol{L}^2(\Omega))} + \|\boldsymbol{J}_\star^{[N]}\|^2_{H^2(\boldsymbol{L}^2(\Omega))}\right].$$

Using Proposition 3.5, we bound:

$$\begin{aligned} M_N(\boldsymbol{E},\boldsymbol{J}) \ &\lesssim\ h^{2s-2}\,\left[\|\boldsymbol{E}^{[N]}\|^2_{H^2(\boldsymbol{X}^{s,q}(\Omega))} + N^{-2\sigma}\,\|\boldsymbol{E}\|^2_{H^2(\boldsymbol{X}^{s,q+\sigma}(\Omega))}\right] \\ &\quad + \tau^2\,\left[\|\boldsymbol{J}^{[N]}\|^2_{H^2(\boldsymbol{L}^2(\Omega))} + N^{-2\sigma}\,\|\boldsymbol{J}\|^2_{H^2(\boldsymbol{H}^{0,\sigma}(\Omega))}\right] \\ &\quad + \tau^2\,\left[\|\boldsymbol{E}^{[N]}\|^2_{H^3(\boldsymbol{L}^2(\Omega))} + N^{-2\sigma}\,\|\boldsymbol{E}\|^2_{H^3(\boldsymbol{H}^{0,\sigma}(\Omega))}\right]. \end{aligned}$$

Then we use the triangle inequality: $\|\boldsymbol{E}_h^{[N];n} - \boldsymbol{E}^n\|_{\boldsymbol{X}}^2 \lesssim \|\boldsymbol{E}_h^{[N];n} - \boldsymbol{E}_\star^{[N];n}\|_{\boldsymbol{X}}^2 + \|\boldsymbol{E}_\star^{[N];n} - \boldsymbol{E}^{[N];n}\|_{\boldsymbol{X}}^2 + \|\boldsymbol{E}^{[N];n} - \boldsymbol{E}^n\|_{\boldsymbol{X}}^2$, and similarly for the L^2 norm of the time derivative. The last two errors are bounded by Propositions 3.3 and 3.6; hence (6.28). The bound (6.29) is obtained in the same manner. □

Remark 6.11. Combining the arguments of Propositions 3.4 and 5.5, we see that the hypotheses:

$$\boldsymbol{\psi} \in H^2(-\delta, T; \boldsymbol{H}^{0,q+\sigma}(\Omega)),\ \ddot{\boldsymbol{E}} \in H^2(-\delta, T; \boldsymbol{H}^{0,q+\sigma}(\Omega)),\ \varrho \in H^2(-\delta, T; \overset{\circ}{H}{}^{1,q+\sigma}(\Omega)),$$

together imply $\boldsymbol{E} \in H^2(-\delta, T; \boldsymbol{X}^{s,q+\sigma}(\Omega))$. The second condition clearly implies $\boldsymbol{E} \in H^4(-\delta, T; \boldsymbol{H}^{0,\sigma}(\Omega))$. In the augmented formulation, the three conditions are satisfied if e.g. $\boldsymbol{J} \in H^4(-\delta, T; \boldsymbol{H}^{0,q+\sigma}(\Omega))$ and $\varrho \in H^3(0, T; \overset{\circ}{H}{}^{1,q+\sigma}(\Omega)) \cap H^5(0, T; H^{-1,s}(\Omega))$. In the mixed augmented formulation, it is enough to have $\boldsymbol{J} \in H^4(-\delta, T; \boldsymbol{H}^{0,q+\sigma}(\Omega))$ and $\varrho \in H^2(0, T; \overset{\circ}{H}{}^{1,q+\sigma}(\Omega)) \cap H^4(0, T; H^{-1,q+\sigma}(\Omega))$.

Remark 6.12. If the Fourier coefficients ϱ^k, $\boldsymbol{J}^k$ are exactly known, it is sufficient to assume $\boldsymbol{E} \in H^2(-\delta, T; \boldsymbol{X}^{s,q}(\Omega)) \cap \mathcal{C}^0(0, T; \boldsymbol{X}^{1,\sigma}(\Omega)) \cap \mathcal{C}^1(0, T; \boldsymbol{H}^{0,\sigma}(\Omega))$ (for $\sigma > 0$) and $\boldsymbol{J} \in H^2(-\delta, T; \boldsymbol{L}^2(\Omega))$.

Remark 6.13. The analyses of §4.3 and Theorem 6.9 can be extended to explicit time schemes. For instance, one can replace the augmented (4.3) and mixed augmented (4.6) formulations with the explicit centred versions:

$$\begin{aligned}(\partial_\tau^2 \boldsymbol{E}_h^{k;n+1} \mid \boldsymbol{F}_h) + a_k(\boldsymbol{E}_h^{k;n}, \boldsymbol{F}_h) \\ = -(\partial_{2\tau} \boldsymbol{J}_\star^{k;n+1} \mid \boldsymbol{F}_h) + (\varrho_\star^{k;n} \mid \operatorname{div} \boldsymbol{F}_h),\end{aligned} \tag{6.30}$$

$$\begin{aligned}\text{resp.}\quad (\partial_\tau^2 \boldsymbol{E}_h^{k;n+1} \mid \boldsymbol{F}_h) + a_k(\boldsymbol{E}_h^{k;n}, \boldsymbol{F}_h) + b_k(\boldsymbol{F}_h, P_h^{k;n+1}) \\ = -(\partial_{2\tau} \boldsymbol{J}_\star^{k;n+1} \mid \boldsymbol{F}_h) + (\varrho_\star^{k;n} \mid \operatorname{div} \boldsymbol{F}_h),\end{aligned} \tag{6.31}$$

which are formally of higher order in time, and computationally very efficient when mass lumping is used. If $\boldsymbol{J}$ is known at the instants $t^{n+1/2}$, the derivative $\partial_{2\tau} \boldsymbol{J}_\star^{k;n+1}$ can be replaced by $\partial_\tau \boldsymbol{J}_\star^{k;n+1/2}$, without changing the order of the scheme.

As in [21], one shows that the L^2-error on the field is indeed of order 2 in τ: provided the fields are regular enough, the estimates (4.10) and (4.20) become respectively:

$$\begin{aligned}\|\boldsymbol{E}_h^{k;n} - \boldsymbol{E}_\star^{k;n}\|_{0,1}^2 \lesssim \epsilon(s,h,k)^2\, \|\boldsymbol{E}_\star^k\|_{H^2(\boldsymbol{X}^s_{(k)}(\omega))}^2 \\ + \tau^4 \left[\|\boldsymbol{E}_\star^k\|_{H^4(\boldsymbol{L}_1^2(\omega))}^2 + \|\boldsymbol{J}_\star^k\|_{H^3(\boldsymbol{L}_1^2(\omega))}^2 \right],\end{aligned} \tag{6.32}$$

$$\begin{aligned}\|\boldsymbol{E}_h^{k;n} - \boldsymbol{E}_\star^{k;n}\|_{0,1}^2 \lesssim (1+k^2)\, \epsilon(s,h,k)^2\, \|\boldsymbol{E}_\star^k\|_{H^2(\boldsymbol{X}^s_{(k)}(\omega))}^2 \\ + \tau^4 \left[\|\boldsymbol{E}_\star^k\|_{H^4(\boldsymbol{L}_1^2(\omega))}^2 + \|\boldsymbol{J}_\star^k\|_{H^3(\boldsymbol{L}_1^2(\omega))}^2 \right].\end{aligned} \tag{6.33}$$

On the other hand, the bounds (4.9) or (4.19) hold without change. Furthermore, all these estimates are valid under the CFL condition $\Lambda\, \tau^2 < 4$, where the Rayleigh quotient $\Lambda := \sup_{\boldsymbol{v}_h \in \mathbb{X}^h_{(k)}} \dfrac{\|\boldsymbol{v}_h\|_{\boldsymbol{X},(k)}^2}{\|\boldsymbol{v}_h\|_{0,1}^2}$ should behave as $\Lambda \lesssim h^{-2} + |k|^2$.

Under the assumptions $\boldsymbol{E} \in H^2(-\delta, T; \boldsymbol{X}^{s,q+\sigma}(\Omega)) \cap H^4(-\delta, T; \boldsymbol{H}^{0,\sigma}(\Omega))$ and $\boldsymbol{J} \in H^3(-\delta, T; \boldsymbol{H}^{0,\sigma}(\Omega))$, where s, q and σ are as in Theorem 6.9, we obtain the bound (6.28) on the reconstructed solution, and the L^2 estimate:

$$\|\boldsymbol{E}_h^{[N];n} - \boldsymbol{E}^n\|_0^2 \le M_3\, (h^{2s-2} + \tau^4 + N^{-2\sigma}). \tag{6.34}$$

But they are valid under a CFL condition strongly dependent on the number of Fourier modes used. Thus, explicit schemes may be difficult to use in practice unless the fields are very regular in θ (i.e. σ is large enough), which allows one to use very few modes.

7. Numerical algorithms

A practical implementation of the SCM in the case where the data are axisymmetric was exposed in [4]. In the case of general data, the method can be applied to the equations of the mode 0. Let us recall the principle of the SCM [5]: the basis of the singular space $\mathbb{X}_{(0)}^{\mathrm{sing};h}$ is computed, once and for all, as a first part of the algorithm, before solving the Maxwell evolution problem in the suitable space $\mathbb{X}_{(0)}^{h} = \mathbb{X}_{(0)}^{\mathrm{reg};h} \oplus \mathbb{X}_{(0)}^{\mathrm{sing};h}$. These various versions of the SCM also take advantage of the following specific points:

- At the mode 0, the Maxwell equations decouple into problems involving the meridian (r, z) and azimuthal (θ) components, which are orthogonal, both in $\boldsymbol{L}_1^2(\omega)$ and $\boldsymbol{X}_{(0)}(\omega)$. Moreover, the azimuthal components are regular and are not affected by the divergence constraint.
- The singular space is spanned by suitably chosen fields: e.g. the gradients of singular functions of the Laplacian, or fields *orthogonal* to the regular space; this yields simple expressions of the various terms coupling the regular and singular parts in the variational formulations.

We now present an extension of this approach to the modes $k \neq 0$. The principle consists in choosing an orthogonal complement (thus $\mathbb{X}_{(k)}^{h} = \mathbb{X}_{(k)}^{\mathrm{reg};h} \overset{\perp}{\oplus} \mathbb{X}_{(k)}^{\mathrm{sing};h}$) for the modes $|k| \leq 2$, while the modes ± 2 serve as the “fundamental modes” for the higher modes $|k| > 2$, thanks to the stabilisation of spaces for these modes (see Proposition 2.9). This is the method already used in [20] for the Poisson problem.

Thus, at the continuous level, the practical decomposition of the solution to Maxwell's equations is chosen as at the end of §6.1:

$$
\begin{aligned}
(7.1)\qquad & \boldsymbol{E}^{k;n} = \boldsymbol{E}^{k;n}_{\mathrm{reg}} + \sum_{\boldsymbol{j}} \kappa_j^{k;n}\, \mathbf{x}_{S\perp}^{\ell(k),j}, \quad \text{where:} \quad \boldsymbol{E}^{k;n}_{\mathrm{reg}} \in \boldsymbol{X}^{\mathrm{reg}}_{(k)}(\omega),\\
& \ell(k) = k \text{ for } |k| \leq 1, \quad \ell(k) = 2\,\mathrm{sign}(k) \text{ for } |k| \geq 2,\\
& \boldsymbol{j} \in \{\boldsymbol{e}, \boldsymbol{c}\} \text{ for } k = 0, \quad \boldsymbol{j} \in \{\boldsymbol{e}\} \text{ for } |k| \geq 1\,;
\end{aligned}
$$

moreover, the basis $(\mathbf{x}_{S\perp}^{k,j})_j$ is orthonormal, and orthogonal to the regular space $\boldsymbol{X}^{\mathrm{reg}}_{(k)}(\omega) = \boldsymbol{X}^{\mathrm{reg}}_{(\ell(k))}(\omega)$ with respect to the form $a_{\ell(k)}(\cdot,\cdot)$.

7.1. Computation of a basis of the singular space $\mathbb{X}_{(k)}^{\mathrm{sing};h}$, for $|k| \leq 2$.

At the discrete level, we define the counterparts of the various terms in (7.1):

$$
(7.2)\qquad \boldsymbol{E}^{k;n}_h = \boldsymbol{E}^{k;n}_{\mathrm{reg};h} + \sum_{\boldsymbol{j}} \kappa_{j;h}^{k;n}\, \mathbf{x}_{S\perp}^{\ell(k),j;h}, \quad \text{where:} \quad \boldsymbol{E}^{k;n}_{\mathrm{reg};h} \in \mathbb{X}^{\mathrm{reg};h}_{(k)},
$$

and the numerical singular fields $\mathbf{x}_{S\perp}^{k,j;h}$ ($|k| \leq 2$) are computed as follows. In the first step, one defines the fields

$$
\mathbf{x}_S^{k,j;h} := \mathbf{S}_j + \widehat{\mathbf{x}}^{k,j;h}, \quad \text{such that} \quad \mathbf{x}_S^{k,j;h} \in \boldsymbol{X}_{(k)}(\omega) \quad \text{and} \quad \mathbf{x}_S^{k,j;h} \perp_{a_k} \mathbb{X}^{\mathrm{reg};h}_{(k)}\,,
$$

i.e. the non-principal part $\widehat{\mathbf{x}}^{k,j;h}$ of the field belongs to the finite element space and satisfies the appropriate variational formulation and boundary conditions, namely:

$$\begin{aligned}
& a_k(\widehat{\mathbf{x}}^{k,j;h}, \boldsymbol{w}_h) = -a_k(\mathbf{S}_j, \boldsymbol{w}_h) \\
& \qquad = -(\mathbf{curl}_k\, \mathbf{S}_j \mid \mathbf{curl}_k\, \boldsymbol{w}_h) - (\mathrm{div}_k\, \mathbf{S}_j \mid \mathrm{div}_k\, \boldsymbol{w}_h), \quad \forall \boldsymbol{w}_h \in \mathbb{X}^{\mathrm{reg};h}_{(k)}\,; \\
& \widehat{\mathbf{x}}^{k,j;h} \times \boldsymbol{n} = -\mathbf{S}_j \times \boldsymbol{n} \text{ on } \gamma_b\,, \quad \text{for } |k| \le 2\,; \\
& \widehat{\mathbf{x}}^{0,j;h} \cdot \mathbf{e}_r = 0 \quad \text{and} \quad \widehat{\mathbf{x}}^{0,j;h} \cdot \mathbf{e}_\theta = 0 \quad \text{on } \gamma_a\,, \\
& \widehat{\mathbf{x}}^{\pm 1,j;h} \cdot \mathbf{e}_\mp = 0 \quad \text{and} \quad \widehat{\mathbf{x}}^{\pm 1,j;h} \cdot \mathbf{e}_z = 0 \quad \text{on } \gamma_a\,, \quad \widehat{\mathbf{x}}^{\pm 2,j;h} = 0 \quad \text{on } \gamma_a.
\end{aligned}$$

Above, we have $\mathbf{curl}_0\, \mathbf{S}_c = 0$ and $\mathrm{div}_0\, \mathbf{S}_c = -\Delta_0[\rho^{\nu_c} P_{\nu_c}(\cos\phi_c)] = 0$, while for the edge singularity:

$$\mathrm{div}_k\, \mathbf{S}_e = -\frac{2\alpha_e}{a_e}\, \rho_e^{\alpha_e - 1} \sin((\alpha_e - 1)\phi_e - \phi_e^0)\,; \tag{7.3}$$

$$\mathbf{curl}_k\, \mathbf{S}_e = \frac{\alpha_e\, \rho_e^{\alpha_e - 1}}{a_e} \begin{pmatrix} -\mathrm{i}k \cos((\alpha_e - 1)\phi_e - \phi_e^0) \\ \cos((\alpha_e - 1)\phi_e - \phi_e^0) \\ \mathrm{i}k \sin((\alpha_e - 1)\phi_e - \phi_e^0) \end{pmatrix}. \tag{7.4}$$

These fields belong to $L^2_1(\omega)$; the corresponding integrals should be computed by an appropriate quadrature formula in the neighbourhood of the corner $\boldsymbol{e}$; elsewhere, the usual mass matrix can be used, cf. [4, §4.4].

At the end of this step, the singular complement $\mathbb{X}^{\mathrm{sing};h}_{(k)}$ is defined as the space generated by the $(\mathbf{x}_S^{k,j;h})_j$, for $|k| \le 2$ and $\boldsymbol{j}$ in the relevant set of singularities. The stabilisation of spaces then allows to set $\mathbb{X}^{\mathrm{sing};h}_{(k)} = \mathbb{X}^{\mathrm{sing};h}_{(2)}$ for $|k| \ge 2$; notice furthermore that $\mathbb{X}^{\mathrm{sing};h}_{(-2)} = \mathbb{X}^{\mathrm{sing};h}_{(2)}$ as we shall see below. Thus, the total space $\mathbb{X}^h_{(k)}$ is spanned by the usual nodal finite elements plus $(\mathbf{S}_e)_e$, for all k, and also plus $(\mathbf{S}_c)_c$, for $k = 0$: we are in the framework of §6, which validates the error estimates.

The second step consists in orthormalising the basis of $\mathbb{X}^{\mathrm{sing};h}_{(k)}$, i.e. one determines the fields

$$\mathbf{x}_{S\perp}^{k,j;h} = \sum_{\boldsymbol{i}} c_i^{k,j;h}\, \mathbf{x}_S^{k,i;h} \quad \text{s.t.} \quad a_k(\mathbf{x}_{S\perp}^{k,i;h}, \mathbf{x}_{S\perp}^{k,j;h}) = \delta_{i,j},$$

for $|k| \le 2$ and $\boldsymbol{i}$, $\boldsymbol{j}$ in the relevant set of singularities. This involves the computation of the scalar products

$$a_k(\mathbf{x}_S^{k,j;h}, \mathbf{x}_S^{k,i;h}) = a_k(\widehat{\mathbf{x}}^{k,j;h}, \widehat{\mathbf{x}}^{k,i;h}) + a_k(\mathbf{S}_j, \widehat{\mathbf{x}}^{k,i;h}) + a_k(\widehat{\mathbf{x}}^{k,j;h}, \mathbf{S}_i) + a_k(\mathbf{S}_j, \mathbf{S}_i);$$

the first term is computed by the stiffness matrix, while the other three need the same treatment near the corners as above. Then the orthonormalisation itself is performed by the usual Schmidt or Arnoldi procedure.

7.2. **Solution of the evolution problem.** The solution of the mixed augmented evolution problem at the mode 0 follows the principle of [4, §4.3], except that we are now using orthogonal complements. As said above, the azimuthal component of $\boldsymbol{E}^0$ is regular; it is solution to a wave-like equation which can be easily solved by nodal finite elements [4, §2.3]. We now expose the solution of the meridian problem. Notice that the orthogonalisation procedure only modifies the meridian components, so the $\mathbf{x}_{S\perp}^{0,j;h}$ are meridian.

We use the following notations: $\mathbf{u} = u_r\,\mathbf{e}_r + u_z\,\mathbf{e}_z$ is the meridian component of $\boldsymbol{u}$; the scalar curl (or *rotational*) and divergence operators of meridian fields are:

$$\operatorname{rot}\mathbf{u} := \partial_r u_z - \partial_z u_r, \quad \operatorname{div}\mathbf{u} := r^{-1}\,\partial_r(r\,u_r) + \partial_z u_z,$$

and the bilinear forms a_0 and b_0 reduce to

$$\mathfrak{a}_0(\mathbf{u},\mathbf{v}) = (\operatorname{rot}\mathbf{u} \mid \operatorname{rot}\mathbf{v}) + (\operatorname{div}\mathbf{u} \mid \operatorname{div}\mathbf{v}), \quad \mathfrak{b}_0(\mathbf{u},p) = (\operatorname{div}\mathbf{u} \mid p).$$

Now, we are able to put the splitting (7.2) (restricted to the meridian components) into the suitable variational formulation. As an example, we show the totally implicit, mixed augmented formulation (4.6)–(4.7), with the time index $n+1$ shifted to n. The adaptation to the non-mixed case is obvious. Taking successively as test functions $\mathbf{F}_h \in \mathbb{X}^{\mathrm{reg};h}_{(0)}$ and $\mathbf{x}^{0,i;h}_{S\perp}$ in (4.6), and then $q_h \in Q_h$ in (4.7), we arrive at the coupled mixed problem:

Find $(\mathbf{E}^{0;n}_{\mathrm{reg};h}, P^{0;n}_h) \in \mathbb{X}^{\mathrm{reg};h}_{(0)} \times Q_h$ *and* $\overrightarrow{\kappa}^{0;n}_h = \left(\kappa^{0;n}_{j;h}\right)_j \in \mathbb{R}^{N_e+N_c}$ ([4]) *such that, for all* $(\mathbf{F}_h, \boldsymbol{i}, q_h) \in \mathbb{X}^{\mathrm{reg};h}_{(0)} \times \{\boldsymbol{e},\boldsymbol{c}\} \times Q_h$*:*

$$\partial^2_\tau\left(\mathbf{E}^{0;n}_{\mathrm{reg};h} \mid \mathbf{F}_h\right) + \sum \partial^2_\tau \kappa^{0;n}_{j;h}\left(\mathbf{x}^{0,j;h}_{S\perp} \mid \mathbf{F}_h\right) + \mathfrak{a}_0\left(\mathbf{E}^{0;n}_{\mathrm{reg};h}, \mathbf{F}_h\right) + \mathfrak{b}_0\left(\mathbf{F}_h, P^{0;n}_h\right) = -\left(\partial_\tau \mathbf{J}^{0;n}_\star \mid \mathbf{F}_h\right) + \left(\varrho^{0;n}_\star \mid \operatorname{div}\mathbf{F}_h\right), \tag{7.5}$$

$$\partial^2_\tau\left(\mathbf{E}^{0;n}_{\mathrm{reg};h} \mid \mathbf{x}^{0,i;h}_{S\perp}\right) + \sum \partial^2_\tau \kappa^{0;n}_{j;h}\left(\mathbf{x}^{0,j;h}_{S\perp} \mid \mathbf{x}^{0,i;h}_{S\perp}\right) + \kappa^{0;n}_{i;h} + \mathfrak{b}_0\left(\mathbf{x}^{0,i;h}_{S\perp}, P^{0;n}_h\right) = -\left(\partial_\tau \mathbf{J}^{0;n}_\star \mid \mathbf{x}^{0,i;h}_{S\perp}\right) + \left(\varrho^{0;n}_\star \mid \operatorname{div}\mathbf{x}^{0,i;h}_{S\perp}\right), \tag{7.6}$$

$$\mathfrak{b}_0\left(\mathbf{E}^{0;n}_{\mathrm{reg};h}, q_h\right) + \sum \kappa^{0;n}_{j;h}\,\mathfrak{b}_0\left(\mathbf{x}^{0,j;h}_{S\perp}, q_h\right) = \left(\varrho^{0;n}_\star \mid q_h\right). \tag{7.7}$$

The summation runs on all singularities $\boldsymbol{j} \in \{\boldsymbol{e},\boldsymbol{c}\}$. The numerical solution of this problem then follows the principle of [4, §4.3].

The method for the modes $k = \pm 1$ is similar, as the singular fields are adapted to these modes. The differences are: the meridian and azimuthal components cannot be decoupled, as they are not orthogonal for the form $a_{\pm 1}(\cdot,\cdot)$, and the boundary condition on the axis γ_a mixes them. Instead, one has to use the basis $(\mathbf{e}_+, \mathbf{e}_-, \mathbf{e}_z)$, as remarked above (cf. Remark 2.7). Moreover, there are no singularities at the sharp vertices. Thus, we arrive at the following formulation:

Find $(\boldsymbol{E}^{k;n}_{\mathrm{reg};h}, P^{k;n}_h) \in \mathbb{X}^{\mathrm{reg};h}_{(k)} \times Q_h$ *and* $\overrightarrow{\kappa}^{k;n}_h = \left(\kappa^{k;n}_{e;h}\right)_e \in \mathbb{R}^{N_e}$ *such that, for all* $(\boldsymbol{F}_h, \boldsymbol{i}, q_h) \in \mathbb{X}^{\mathrm{reg};h}_{(k)} \times \{\boldsymbol{e}\} \times Q_h$*:*

$$\partial^2_\tau\left(\boldsymbol{E}^{k;n}_{\mathrm{reg};h} \mid \boldsymbol{F}_h\right) + \sum \partial^2_\tau \kappa^{k;n}_{e;h}\left(\mathbf{x}^{k,e;h}_{S\perp} \mid \boldsymbol{F}_h\right) + a_k\left(\boldsymbol{E}^{k;n}_{\mathrm{reg};h}, \boldsymbol{F}_h\right) + b_k\left(\boldsymbol{F}_h, P^{k;n}_h\right) = -\left(\partial_\tau \boldsymbol{J}^{k;n}_\star \mid \boldsymbol{F}_h\right) + \left(\varrho^{k;n}_\star \mid \operatorname{div}_k \boldsymbol{F}_h\right), \tag{7.8}$$

$$\partial^2_\tau\left(\boldsymbol{E}^{k;n}_{\mathrm{reg};h} \mid \mathbf{x}^{k,i;h}_{S\perp}\right) + \sum \partial^2_\tau \kappa^{k;n}_{e;h}\left(\mathbf{x}^{k,e;h}_{S\perp} \mid \mathbf{x}^{k,i;h}_{S\perp}\right) + \kappa^{k;n}_{i;h} + b_k\left(\mathbf{x}^{k,i;h}_{S\perp}, P^{k;n}_h\right) = -\left(\partial_\tau \boldsymbol{J}^{k;n}_\star \mid \mathbf{x}^{k,i;h}_{S\perp}\right) + \left(\varrho^{k;n}_\star \mid \operatorname{div}_k \mathbf{x}^{k,i;h}_{S\perp}\right), \tag{7.9}$$

$$b_k\left(\boldsymbol{E}^{k;n}_{\mathrm{reg};h}, q_h\right) + \sum \kappa^{k;n}_{e;h}\, b_k\left(\mathbf{x}^{k,e;h}_{S\perp}, q_h\right) = \left(\varrho^{k;n}_\star \mid q_h\right). \tag{7.10}$$

This time, the summation runs on the reentrant edges $\boldsymbol{e}$ only.

---

[4] N_e and N_c are the numbers of reentrant edges and sharp vertices.

We now examine the cases of the modes $|k| \geq 2$. First, we show that the meridian and azimuthal components are orthogonal w.r.t. the form $a_k(\cdot,\cdot)$. Let $\boldsymbol{u}$, $\boldsymbol{v}$ be vector fields in the space

$$\boldsymbol{H}_{(k)}(\mathbf{curl}_k, \mathrm{div}_k; \omega) := \left\{\boldsymbol{w} \in \boldsymbol{L}^2_{-1}(\omega) : \mathbf{curl}_k\, \boldsymbol{w} \in \boldsymbol{L}^2_1(\omega) \text{ and } \mathrm{div}_k\, \boldsymbol{w} \in L^2_1(\omega)\right\}.$$

A simple integration by parts shows

$$\begin{aligned} a_k(\boldsymbol{u},\boldsymbol{v}) &= \mathfrak{a}_0(\mathbf{u},\mathbf{v}) + k^2\left(\frac{\mathbf{u}}{r} \;\Big|\; \frac{\mathbf{v}}{r}\right) \\ &\quad + (\mathbf{curl}\, u_\theta \mid \mathbf{curl}\, v_\theta) + k^2\left(\frac{u_\theta}{r} \;\Big|\; \frac{v_\theta}{r}\right) + \mathrm{i}k\, B(\boldsymbol{u},\boldsymbol{v}) \\ &:= \mathfrak{a}_k(\mathbf{u},\mathbf{v}) + \mathsf{a}_k(u_\theta, v_\theta) + \mathrm{i}k\, B(\boldsymbol{u},\boldsymbol{v}), \end{aligned} \tag{7.11}$$

where the vector $\mathbf{curl}$ of a scalar field is defined as $\mathbf{curl}\, w := -\partial_z w\, \mathbf{e}_r + r^{-1}\, \partial_r(r\, w)\, \mathbf{e}_z$. Thanks to the absence of singularities at the sharp vertices, the fields in $\boldsymbol{X}_{(k)}(\omega)$ are of $\boldsymbol{H}^1_{(k)}$ regularity near the axis, and thus automatically belong to $\in \boldsymbol{L}^2_{-1}(\omega)$. (The same holds for the magnetic boundary condition). The boundary term $B(\boldsymbol{u},\boldsymbol{v})$ is equal to

$$B(\boldsymbol{u},\boldsymbol{v}) = \int_{\gamma_b} \{(\boldsymbol{u}\cdot\boldsymbol{n})\,\overline{v}_\theta - u_\theta\,(\overline{\boldsymbol{v}}\cdot\boldsymbol{n})\}\,\mathrm{d}\gamma,$$

so it vanishes when $\boldsymbol{u}\times\boldsymbol{n} = \boldsymbol{v}\times\boldsymbol{n} = 0$ (and likewise when $\boldsymbol{u}\cdot\boldsymbol{n} = \boldsymbol{v}\cdot\boldsymbol{n} = 0$). As far as the form b_k is concerned, there holds:

$$b_k(\boldsymbol{u}, p) = \mathfrak{b}_0(\mathbf{u}, p) + \mathrm{i}k\left(\frac{u_\theta}{r} \;\Big|\; p\right).$$

Unlike the mode 0, the divergence constraint mixes the meridian and azimuthal components. Fully decoupling these components is therefore possible in the non-mixed formulation (4.3) only.

The formula (7.11) has several consequences. First, $a_k = a_{-k}$, so the orthogonalisation procedure of §7.1 gives $\mathbf{x}^{-2,e;h}_{S\perp} = \mathbf{x}^{2,e;h}_{S\perp}$. Moreover, given that the azimuthal component of $\mathbf{S}_e$ is zero, and the azimuthal component of any field in $\boldsymbol{X}_{(k)}(\omega)$ is regular (recall the proof of Proposition 2.9), the orthogonalisation procedure only modifies the meridian components of $\mathbf{S}_e$, and so the $\mathbf{x}^{2,e;h}_{S\perp}$ are meridian. Finally, there holds:

$$a_k(\boldsymbol{u},\boldsymbol{v}) = a_2(\boldsymbol{u},\boldsymbol{v}) + (k^2-4)\left(\frac{\boldsymbol{u}}{r} \;\Big|\; \frac{\boldsymbol{v}}{r}\right) := a_2(\boldsymbol{u},\boldsymbol{v}) + (k^2-4)\,[\boldsymbol{u} \mid \boldsymbol{v}]_{-1}. \tag{7.12}$$

If we take successively as test functions $\boldsymbol{F}_h \in \mathbb{X}^{\mathrm{reg};h}_{(k)}$ and $\mathbf{x}^{0,i;h}_{S\perp}$ in (4.6), and take into account the orthogonality of the basis $\left(\mathbf{x}^{2,e;h}_{S\perp}\right)_e$ for the form a_2, we arrive at the coupled mixed problem:

Find $(\boldsymbol{E}^{k;n}_{\mathrm{reg};h}, P^{k;n}_h) \in \mathbb{X}^{\mathrm{reg};h}_{(k)} \times Q_h$ *and* $\overrightarrow{\kappa}^{k;n}_h = \left(\kappa^{k;n}_{e;h}\right)_e \in \mathbb{R}^{N_e}$ *such that, for all*

$(\boldsymbol{F}_h, \boldsymbol{i}, q_h) \in \mathbb{X}_{(k)}^{\mathrm{reg};h} \times \{\boldsymbol{e}\} \times Q_h$:

$$\begin{aligned}(7.13)\qquad &\partial_\tau^2 \left(\boldsymbol{E}_{\mathrm{reg};h}^{k;n} \mid \boldsymbol{F}_h\right) + \sum \partial_\tau^2 \kappa_{e;h}^{k;n} \left(\mathbf{x}_{S\perp}^{2,e;h} \mid \boldsymbol{F}_h\right) + a_k \left(\boldsymbol{E}_{\mathrm{reg};h}^{k;n}, \boldsymbol{F}_h\right) \\ &+ (k^2-4) \sum \kappa_{e;h}^{k;n} \left[\mathbf{x}_{S\perp}^{2,e;h} \mid \boldsymbol{F}_h\right]_{-1} + b_k \left(\boldsymbol{F}_h, P_h^{k;n}\right) \\ &= -\left(\partial_\tau \boldsymbol{J}_\star^{k;n} \mid \boldsymbol{F}_h\right) + \left(\varrho_\star^{k;n} \mid \operatorname{div}_k \boldsymbol{F}_h\right),\end{aligned}$$

$$\begin{aligned}(7.14)\qquad &\partial_\tau^2 \left(\boldsymbol{E}_{\mathrm{reg};h}^{k;n} \mid \mathbf{x}_{S\perp}^{2,i;h}\right) + \sum \partial_\tau^2 \kappa_{e;h}^{k;n} \left(\mathbf{x}_{S\perp}^{2,e;h} \mid \mathbf{x}_{S\perp}^{2,i;h}\right) + \kappa_{i;h}^{k;n} \\ &+ (k^2-4) \sum \kappa_{e;h}^{k;n} \left[\mathbf{x}_{S\perp}^{2,e;h} \mid \mathbf{x}_{S\perp}^{2,i;h}\right]_{-1} + \mathfrak{b}_0 \left(\mathbf{x}_{S\perp}^{2,i;h}, P_h^{k;n}\right) \\ &= -\left(\partial_\tau \boldsymbol{J}_\star^{k;n} \mid \mathbf{x}_{S\perp}^{2,i;h}\right) + \left(\varrho_\star^{k;n} \mid \operatorname{div}_k \mathbf{x}_{S\perp}^{2,i;h}\right),\end{aligned}$$

$$(7.15)\qquad b_k \left(\boldsymbol{E}_{\mathrm{reg};h}^{k;n}, q_h\right) + \sum \kappa_{e;h}^{k;n}\, \mathfrak{b}_0 \left(\mathbf{x}_{S\perp}^{2,e;h}, q_h\right) = \left(\varrho_\star^{k;n} \mid q_h\right).$$

The summation runs on the reentrant edges $\boldsymbol{e}$.

From a numerical point of view, notice that the various terms in (7.5–7.7), (7.8–7.10), and (7.13–7.15) involving the $\mathbf{x}_{S\perp}^{k,j;h}$ correspond to integrals with singular integrands near the geometrical singularities; similarly, the integrals defining the forms $a_k(\cdot,\cdot)$ and $[\cdot \mid \cdot]_{-1}$ need special care near the axis γ_a. See [4, §4.4] for an efficient implementation.

7.3. **Miscellaneous.** Let us now explain briefly the decoupling of meridian and azimuthal components in the non-mixed formulation.

The meridian component $\mathbf{E}_{\mathrm{reg};h}^{k;n}$ is solution to a problem similar to (7.13)–(7.14), without the b_k and $\mathfrak{b}_0$ terms, and with div instead of div_k.

As for the azimuthal component, we recall that it is regular. Indeed, at the continuous level, $E^k := E_\theta^k$ belongs to $H_{(k)}^1(\omega) \cap \overset{\diamond}{H}{}_1^1(\omega) = V_1^1(\omega) \cap \overset{\diamond}{H}{}_1^1(\omega)$, and is solution to (cf. (2.31)):

$$(7.16)\quad \left\langle \ddot{E}^k, F\right\rangle + \mathsf{a}_k(E^k, F) = -\left(j^k \mid F\right) + \mathrm{i}k \left(\frac{\varrho^k}{r} \;\middle|\; F\right), \quad \forall F \in V_1^1(\omega) \cap \overset{\diamond}{H}{}_1^1(\omega).$$

This is a wave-like equation whose strong form writes:

$$\partial_t^2 E^k - \Delta_1 E^k + (k^2/r^2)\, E^k = -\partial_t J^k + (\mathrm{i}k/r)\, \varrho^k\,;$$

its numerical solution by nodal finite elements is no difficulty. The azimuthal components of fields in $\mathbb{X}_{(k)}^h$ belong to

$$V_\circ^h = \left\{w_h \in \mathcal{C}^0(\overline{\varpi})^3 : v_{h|T} \in \mathbb{P}_\kappa(T),\ \forall T \in \mathcal{T}_h,\ \text{and } v_{h|\partial\omega} = 0\right\}.$$

Taking an azimuthal test function in (4.3), we arrive at the following formulation:

$$\partial_\tau^2 \left(E_h^{k;n} \mid F_h\right) + \mathsf{a}_k(E_h^{k;n}, F_h) = -\left(\partial_\tau J_\star^{k;n} \mid F_h\right) + \mathrm{i}k \left(\frac{\varrho_\star^{k;n}}{r} \;\middle|\; F_h\right) \quad \forall F_h \in V_\circ^h.$$

Finally, we show that the overall cost of the method can be slightly reduced, as in [19, 20], by setting $\kappa_{e;h}^{k;n} := 0$ for $|k|$ large enough, i.e., setting $\boldsymbol{E}_h^{k;n} := \boldsymbol{E}_{\mathrm{reg};h}^{k;n}$,

where $\boldsymbol{E}^{k;n}_{\mathrm{reg};h}$ is the solution to the mixed augmented problem:
Find $(\boldsymbol{E}^{k;n}_{\mathrm{reg};h}, P^{k;n}_h) \in \mathbb{X}^{\mathrm{reg};h}_{(k)} \times Q_h$ *such that, for all* $(\boldsymbol{F}_h, q_h) \in \mathbb{X}^{\mathrm{reg};h}_{(k)} \times Q_h$*:*

$$\partial^2_\tau \left(\boldsymbol{E}^{k;n}_{\mathrm{reg};h} \mid \boldsymbol{F}_h\right) + a_k \left(\boldsymbol{E}^{k;n}_{\mathrm{reg};h}, \boldsymbol{F}_h\right) + b_k \left(\boldsymbol{F}_h, P^{k;n}_h\right) = - \left(\partial_\tau \boldsymbol{J}^{k;n}_\star \mid \boldsymbol{F}_h\right) + \left(\varrho^{k;n}_\star \mid \mathrm{div}_k\, \boldsymbol{F}_h\right), \tag{7.17}$$

$$b_k \left(\boldsymbol{E}^{k;n}_{\mathrm{reg};h}, q_h\right) = \left(\varrho^{k;n}_\star \mid q_h\right), \tag{7.18}$$

or of the similar explicit centred or non-mixed versions.

To see that this can be done without deteriorating the convergence rate, we remark that $|\kappa^{k;n}_{e;h}| \lesssim |\lambda^{k;n}_{e;h}|$, where $\lambda^{k;n}_{e;h}$ is the singularity coefficient of $\boldsymbol{E}^{k;n}_h$ defined as in (5.5). Then, using (5.7) and (7.12), we bound:

$$\begin{aligned} \|\boldsymbol{E}^{k;n}_h - \boldsymbol{E}^{k;n}_{\mathrm{reg};h}\|^2_{\boldsymbol{X},(k)} &\lesssim \sum \left|\kappa^{k;n}_{e;h}\right|^2 \|\mathbf{x}^{2,e;h}_{S\perp}\|^2_{\boldsymbol{X},(k)} \\ &\lesssim \sum |k|^{2\alpha_e-2} \|\boldsymbol{E}^{k;n}_h\|^2_{\boldsymbol{X},(k)} \left[1 + (k^2-4)\, \|\mathbf{x}^{2,e;h}_{S\perp}\|^2_{0,-1}\right] \\ &\lesssim |k|^{2\alpha^\star} \|\boldsymbol{E}^{k;n}\|^2_{\boldsymbol{X},(k)}, \end{aligned}$$

where $\alpha^\star = \max_e\{\alpha_e < 1\}$ (the maximum runs over reentrant edges). The squared error of the SCM is controlled by $h^{2s-2}\,|k|^{2q}$, where $q = s$ in the non-mixed case and $q = 1+s$ in the mixed case, if one recalls the required regularity of the electric field in Theorem 6.9. Thus, one can neglect the singular part provided that

$$|k|^{\alpha^\star} \lesssim h^{s-1}\,|k|^q, \quad \text{i.e.} \quad |k| \ge C_\star\, h^{-\frac{s-1}{q-\alpha^\star}}, \text{ for some constant } C_\star.$$

As $\alpha^\star < 1$, we see that the exponent of h, viz. $-\frac{s-1}{q-\alpha^\star}$, is always less than 1 in absolute value.

References

1. C. Amrouche, C. Bernardi, M. Dauge, V. Girault. Vector potentials in three-dimensional non-smooth domains. *Math. Meth. Appl. Sci.* **21**, 823–864 (1998).
2. F. Assous, P. Ciarlet, Jr., S. Labrunie. Theoretical tools to solve the axisymmetric Maxwell equations. *Math. Meth. Appl. Sci.* **25**, 49–78 (2002).
3. F. Assous, P. Ciarlet, Jr., S. Labrunie. Solution of axisymmetric Maxwell equations. *Math. Meth. Appl. Sci.* **26**, 861–896 (2003).
4. F. Assous, P. Ciarlet Jr., S. Labrunie, J. Segré. Numerical solution to the time-dependent Maxwell equations in axisymmetric singular domains: The Singular Complement Method. *J. Comput. Phys.* **191**, 147–176 (2003).
5. F. Assous, P. Ciarlet, Jr., J. Segré. Numerical solution to the time-dependent Maxwell equations in two-dimensional singular domains: The Singular Complement Method. *J. Comput. Phys.* **161**, 218–249 (2000).
6. F. Assous, P. Degond, E. Heintzé, P.A. Raviart, J. Segré. On a finite element method for solving the three-dimensional Maxwell equations. *J. Comput. Phys.* **109**, 222–237 (1993).
7. R. Barthelmé, P. Ciarlet, Jr., E. Sonnendrücker. Generalized formulations of Maxwell's equations for numerical Vlasov–Maxwell equations. *Math. Models Meth. App. Sci.* **17**, 657–680 (2007).
8. Z. Belhachmi, C. Bernardi, S. Deparis. Weighted Clément operator and application to the finite element discretization of the axisymmetric Stokes problem. *Numer. Math.* **105**, 217–247 (2006).
9. Z. Belhachmi, C. Bernardi, S. Deparis, F. Hecht. A truncated Fourier/finite element discretization of the Stokes equations in an axisymmetric domain. *Math. Models Meth. App. Sci.* **16**, 233–263 (2006).

10. F. Ben Belgacem, C. Bernardi. Spectral element discretization of the Maxwell equations. *Math. Comp.* **68**, 1497–1520 (1999).
11. F. Ben Belgacem, C. Bernardi, F. Rapetti. Numerical analysis of a model for an axisymmetric guide for electromagnetic waves. I. The continuous problem and its Fourier expansion. *Math. Methods Appl. Sci.* **28**, 2007–2029 (2005).
12. C. Bernardi, M. Dauge, Y. Maday. *Spectral methods for axisymmetric domains.* Series in Applied Mathematics, Gauthier-Villars, Paris and North Holland, Amsterdam, 1999.
13. M.Sh. Birman, M.Z. Solomyak. The Maxwell operator in regions with nonsmooth boundary. *Siberian Math. J.* **28**, 12–24 (1987).
14. A.-S. Bonnet-Ben Dhia, C. Hazard, S. Lohrengel. A singular field method for the solution of Maxwell's equations in polyhedral domains. *SIAM J. Appl. Math.* **59**, 2028–2044 (1999).
15. S.C. Brenner, J. Cui, F. Li, L.-Y. Sung. A nonconforming finite element method for a two-dimensional curl-curl and grad-div problem. *Numer. Math.* **109**, 509–533 (2008).
16. C. Canuto, A. Quarteroni. Approximation results for orthogonal polynomials in Sobolev spaces. *Math. Comp.* **38**, 67–86 (1982).
17. Z. Chen, Q. Du, J. Zou. Finite element methods with matching and nonmatching meshes for Maxwell equations with discontinuous coefficients. *SIAM J. Numer. Anal.* **37**, 1542–1570 (2000).
18. P. Ciarlet, Jr., V. Girault. Condition *inf-sup* pour l'élément fini de Taylor–Hood P_2-iso-P_1, 3-D; application aux équations de Maxwell. *C. R. Acad. Sci. Paris Ser. I* **335**, 827–832 (2002).
19. P. Ciarlet, Jr., B. Jung, S. Kaddouri, S. Labrunie, J. Zou. The Fourier–Singular Complement Method for Poisson's equation. Part I: prismatic domains. *Numer. Math.* **101**, 423–450 (2005).
20. P. Ciarlet, Jr., B. Jung, S. Kaddouri, S. Labrunie, J. Zou. The Fourier–Singular Complement Method for Poisson's equation. Part II: axisymmetric domains. *Numer. Math.* **102**, 583–610 (2006).
21. P. Ciarlet Jr., S. Labrunie. Numerical analysis of the generalized Maxwell equations (with an elliptic correction) for charged particle simulations. *Math. Models Methods Appl. Sci.* **19**, 1959–1994 (2009).
22. P. Ciarlet Jr., F. Lefèvre, S. Lohrengel, S. Nicaise. Weighted regularization for composite materials in electromagnetism.
To appear in *Modél. Math. Anal. Num.*
23. P. Ciarlet Jr., J. Zou. Fully discrete finite element approaches for time-dependent Maxwell's equations. *Numer. Math.* **82**, 193–219 (1999).
24. D.M. Copeland, J. Gopalakrishnan, J.E. Pasciak. A mixed method for axisymmetric div-curl systems. *Math. Comp.* **77**, 1941–1965 (2008).
25. M. Costabel, M. Dauge. Singularities of Maxwell's equations on polyhedral domains, *in* M. Bach, C. Constanda, G.C. Hsiao *et al.* (eds), *Analysis, Numerics and Applications of Differential and Integral Equations.* Pitman Research Notes in Mathematics Series **379**, Addison-Wesley, Londres, 1998, pp. 69–76.
26. M. Costabel, M. Dauge. Maxwell and Lamé eigenvalues on polyhedra. *Math. Meth. Appl. Sci.* **22**, 243–258 (1999).
27. M. Costabel, M. Dauge. Weighted regularization of Maxwell equations in polyhedral domains. A rehabilitation of nodal finite elements. *Numer. Math.* **93**, 239–277 (2002).
28. M. Costabel, M. Dauge. Computation of resonance frequencies for Maxwell equations in non smooth domains. In Computational Methods for Wave Propagation in Direct Scattering, *Lecture Notes in Comp. Sc. and Eng.* **31**, Springer, Berlin, 2003.
29. M. Costabel, M. Dauge, S. Nicaise. Singularities of Maxwell interface problems. *Modél. Math. Anal. Num.* **33**, 627–649 (1999).
30. M. Dauge, M. Pogu. Existence et régularité de la fonction potentiel pour des écoulements subcritiques s'établissant autour d'un corps à singularité conique. *Annales Fac. Sci. Toulouse* **IX**, 213–242 (1988).
31. V. Girault, P.-A. Raviart. *Finite element method for Navier–Stokes equations.* Springer, Berlin, 1986.
32. C. Hazard, S. Lohrengel. A singular field method for Maxwell's equations: numerical aspects for 2D magnetostatics. *SIAM J. Numer. Anal.* **40** 1021–1040 (2002).

33. B. Heinrich. The Fourier-finite element method for Poisson's equation in axisymmetric domains with edges. *SIAM J. Numer. Anal.* **33**, 1885–1911 (1996).
34. B. Heinrich, S. Nicaise, B. Weber. Elliptic interface problems in axisymmetric domains II: Convergence analysis of the Fourier-finite element method. *Adv. Math. Sci. Appl.* **10**, 571–600 (2003).
35. J.S. Hestaven, T. Warburton. *Nodal discontinuous Galerkin methods.* Texts in Applied Mathematics **54**, Springer, 2008.
36. J.L. Lions, E. Magenes. *Problèmes aux limites non homogènes et applications.* Dunod, Paris, 1968.
37. S. Lohrengel, S. Nicaise. Singularities and density problems for composite materials in electromagnetism. *Comm. P. D. E.* **27**, 1575–1623 (2002).
38. S. Lohrengel, S. Nicaise. A discontinuous Galerkin method on refined meshes for the two-dimensional time-harmonic Maxwell equations in composite materials. *J. Comput. Appl. Math.* **206**, 27–54 (2007).
39. B. Mercier, G. Raugel. Résolution d'un problème aux limites dans un ouvert axisymétrique par éléments finis en r, z et séries de Fourier en θ. *RAIRO Anal. Numér.* **16**, 405–461 (1982).
40. P. Monk. *Finite elements methods for Maxwell's equations.* Oxford Science Publications, 2003.
41. J.-C. Nédélec. Mixed finite elements in $\mathbb{R}^3$, *Numer. Math.* **35**, pp. 315-341 (1980).
42. J.-C. Nédélec. A new family of mixed finite elements in $\mathbb{R}^3$, *Numer. Math.* **50**, pp. 57-81 (1986).
43. B. Nkemzi. Optimal convergence recovery for the Fourier-finite-element approximation of Maxwell's equations in nonsmooth axisymmetric domains. *Applied Numerical Mathematics* **57**, 989–1007 (2007).
44. C. Weber. A local compactness theorem for Maxwell's equations. *Math. Meth. Appl. Sci.* **2**, 12–25 (1980).

Laboratoire POEMS, UMR 7231 CNRS/ENSTA/INRIA, ENSTA ParisTech, 32, boulevard Victor, 75739 Paris Cedex 15, France
E-mail address: `ciarlet@ensta.fr`

Institut Élie Cartan (Mathématiques) UMR 7502, Nancy-Université, CNRS and INRIA (project CALVI), 54056 Vandœuvre-lès-Nancy cedex, France
E-mail address: `labrunie@iecn.u-nancy.fr`